

# 2013

### 4th Year Dissertation



An investigation into the thermal properties of Corex slag and the relationship between thermal profiles and setting times

Prepared by: Kyle van der Westhuizen

Prepared for: Prof Mark Alexander

Student no: VWSKYL001

### **Plagiarism Declaration**

- 1. I know that plagiarism is wrong. Plagiarism is using another's work and to pretend that it is one's own.
- 2. I have used the Harvard Convention for citation and referencing. Each significant contribution to, and quotation in, this report from the work, or works of other people has been attributed and has been cited and referenced.
- 3. This report is my work.
- 4. I have not allowed, and will not allow, anyone to copy our work with the intention of passing it off as his or her own work.
- 5. I acknowledge that copying someone else's assignment or essay, or part of it, is wrong, and declares that this is our own work.

Signed: Kyle van der Westhuizen

### Acknowledgments

I would firstly like to acknowledge Prof. Alexander for his time, guidance and for stimulating a curiosity in the field of cement and concrete technology which will certainly set me in good stead going into the future. Thanks are given to Prof. Moyo for making the necessary equipment available and for his time given in helping with the configuration. Special thanks are given to the PhD students Gladwell Nganga and Matongo Kabani for their time and help in accessing resources. I would also like to acknowledge the Structures Department of Stellenbosch University for allowing the loan of equipment at such short notice. Appreciation is also given to all the lab staff for all their assistance. Finally I would like to thank my family for providing me with the gift of an education.

#### **Abstract**

The heat released due to the exothermic reaction between water and cement, known as the heat of hydration, is of interest due the potential formation of thermally induced cracks resulting from temperature differentials that form stresses during the hardening of early-age concrete. Apart from the formation of thermal cracks, the heat of hydration is also of interest with regard to the time of set and strength development over time, as the heat of hydration is directly related to the chemical reactions that take place within concrete to develop its rigid structure over the curing period.

A new slag extender was introduced into the Western Cape market in 1999 under the name of ground granulated Corex slag (GGCS), and was been found to have a higher reactivity than ordinary blastfurnace slag (GGBS), when supplemented with Portland cement (PC). The higher reactivity has led to the production of superior concretes, with improvements in both strength and durability. However the higher reactivity of Corex slags is couple with an elevated heat of hydration when compared to blastfurnace slag.

The thermal profiles of Corex slag and blastfurnace slag mixed in a proportion of 50% with PC (CEM I 52.5 N) were investigated using a semi-adiabatic method of calorimetry. Based on paste samples blastfurnace slag showed a 46% reduction in the peak temperature of 100% PC compared to 32% offered by Corex slag. The increased reactivity of Corex slag did show higher heat development than blastfurnces slag but a significant reduction in heat is still offered when a comparison is made with 100% PC. However it is important to note that temperature measurements were taken over a 24 hours period under semi-adiabatic conditions. In order to establish temperature profiles to determine quantifiable heat generation a 'fully' adiabatic calorimeter is required. Therefore, due to heat losses, semi-adiabatic calorimetry is only useful for comparative analysis between samples. The variability of parameters associated with semi-adiabatic systems, such as the degree of insulation, requires that the system be tailored and calibrated to specific test objectives.

The setting times of the samples were also determined using SANS 50196-3 (2006) and both slags showed increased setting times, which is expected as slags are latent hydraulic binders. No clear difference in initial setting time was found between the two slags; however the final time of set for Corex slag sample occurred 30 min earlier, which reaffirmed the higher reactivity of Corex slag.

An attempt was made to establish a relationship between the temperature profiles and the measured setting times. The relationship was to be established through determining the proportions of the main peak response (MPR) that corresponded with the setting times, which is known as the fractions method. However the setting times of the experimental mixtures corresponded to very lower proportions of the main peak response resulting in inconclusive correlations, which could be attributed to the high level of insulation provided by the semi-adiabatic calorimetric setup. The insulation was cited as being problematic as the fractions method was established by measuring temperature profiles under relatively low levels of insulation. In an attempt to limit heat loss, to allow for reactivity comparisons, an excessive amount of insulation may have amplified the MPR nullifying the fractions method of determining setting time.

### **Table of Contents**

Plagiaris	m Declaration	I
Acknowl	edgments	II
Abstract		III
Table of	Contents	IV
List of Ta	ables	VI
List of Fi	gures	VI
List of eq	uations	VIII
_	oduction	
	Background and context	
	Problem statement	
1.3	Objectives	
	Justification of study	
1.5	Scope and limitations	
1.6	Outline of dissertation	
2 Lite	rature Review	4
2.1	Cementitious materials	4
2.1.1		
2.1.2	Manufacturing process	4
2.1.3	Cement Extenders	5
2.1.4	Hydration	7
2.1.5	Heat liberation through hydration of cement	8
2.1.6	Setting and hardening of concrete	9
2.1.7	Curing	9
2.1.8	Common cements	9
2.1.9	Cement for concrete	10
2.1.1	0 Water:cement ratio (W/C)	11
2.1.1		
2.2	Corex and blastfurnace slags	
2.2.1	Slag characterisation	
2.2.2	$\epsilon$	
2.2.3		
2.2.4		
2.2.5	, ,	
2.2.6	2,	
2.2.7		
2.2.8		
<b>2.3</b> 2.3.1	Thermal properties	
2.3.1	Thermal properties	
2.3.2		
2.3.4	1	
	Determination of heat liberation in cementitious binders	

	2.4.1	Isothermal calorimetry	24
	2.4.2	Semi-adiabatic calorimetry	25
	2.4.3	Adiabatic calorimetry	26
	2.4.4	ASTM thermal measuring <u>draft</u> standard	27
	2.4.5	Conclusion	
	2.5	Predicting temperature in early age concrete	31
	2.5.1	Conclusion	35
	2.6	Methods of assessing setting time	35
	2.6.1	SANS 50196-3:2006	35
	2.6.2	ASTM C403/C403M - 08	35
	2.7	Main findings of literature	37
3	Exp	erimental methodology	38
	3.1	Cement paste proportion	38
	3.2	Standard consistence and time of setting	38
	3.2.1	Summary of experimental procedure	38
	3.3	Calorimetry method	39
	3.4	Cost breakdown of semi-adiabatic calorimetric system	40
4	Resi	ılts	42
	4.1	Standard consistence and time of setting	42
	4.1.1	Standard consistence test	42
	4.1.2	Initial and final setting time	42
	4.2	Semi-adiabatic calorimetry	44
	4.2.1	Temperature profiles	44
	4.2.2	Heat profiles	47
	4.2.3	Rate of heat evolution	50
	4.3	Temperature profile and setting time relationship	53
	4.4	Heat rate profile and setting time relationship	55
5	Con	clusions	57
	5.1	Thermal properties of GGCS and GGBS	57
	5.2	Semi-adiabatic calorimetry	57
	5.3	Setting time properties of GGCS and GGBS	58
	5.4	Relationship between thermal profile and setting time	58
6	Refe	rence list	59
7	App	endix A – Standard consistence and setting time experimental detail	62
	7.1	Apparatus	
	7.2	Procedure	62
8	App	endix B – Semi-adiabatic calorimetric experimental procedure	65
	8.1	Apparatus	
	8.2	Procedure	

### **List of Tables**

Table 2-1 Primary raw materials of PC (Owens, 2012)	4
Table 2-2 Primary raw materials of PC (Fulton, 2012, p.22)	5
Table 2-3 Effects of extenders on concrete properties (Grieve, 2009, p.4)	
Table 2-4 Permitted products in SANS 50197-1 (Owens, 2012, p.29)	
Table 2-5 Oxide analysis of PC, GGBS and GGCS, % by mass (Jaufeerally, 2002).	12
Table 2-6 Physical properties of PC, GGBS and GGCS (Alexander et al., 2003, p.9	
Table 2-7 Intial and final setting time for standard cementitious pastes (Alexar	nder et al.,
2003, p.14)	14
Table 2-8 Characteristics of durability indexes	16
Table 3-1 Proportions of experiment mixtures	38
Table 3-2 Estimated cost breakdown of semi-adiabatic calorimetric system	40
Table 4-1 w/b ratio at standard consistence and corresponding Blaine fineness	42
Table 4-2 Initial and final setting times of experimental mixtures	43
Table 4-3 Setting time results with CEM I 42.5 N and variation from CEM	I 52.5 N
(Jaufeerally, 2002)	
Table 4-4 Signal-to-Noise ratio of the experimental mixers	
Table 4-5 Peak temperature and the percentage change from 100% PC due to 0	
GGCS additions	
Table 4-6 Peak heat rates and the percentage change from 100% PC due to slag add	lition50
Table 4-7 Proportion of main peak response corresponding to initial and final se	tting times
for temperature profiles	53
Table 4-8 Proportion of main peak response corresponding to initial and final se	tting times
for heat rate profiles	55
List of Figures	
Figure 2-1 Structure of hardened concrete paste (Grieve, 2009)	8
Figure 2-2 Classification stages of hydration developed by isothermal calorim	
1989)	
Figure 2-3 Relationship between water:cement ratio and concrete compressive st	
different cement strengths using crushed aggregate (Kishore, 2010)	C
Figure 2-4 Compressive strength of GGBS (left) and GGCS (right) as function	
replacement and w/b ratio (Alexander et al., 2003, pp.12-13)	_
Figure 2-5 Bleeding characteristics of concrete for varying Corex slag contents, w	
Figure 2-5 Directing characteristics of concrete for varying corex stag contents, $w = 0.4$ and (b) $w/b = 0.6$ (Alexander et al., 2003, p.15)	
Figure 2-6 Total heat produced during hydration for different slag binder con	
(Alexander et al., 2003, p.17)	
· · · · · · · · · · · · · · · · · · ·	
Figure 2-7 Iso-index charts for Corex slag concretes (Alexander et al., 2003, p.23). Figure 2-8 Material costs (Rands/m³) of concrete for different concrete grades (Alexander et al., 2004, p.23).	
al., 2003, p.27)	
_	
Figure 2-9 Material cost (Rands/m <sup>3</sup> ) for severe marine environment (Alexander et	
p.27)	19

Figure 2-10 Thermal conductivity variations during the early stages of hydration (Ballim & Graham, 2009, p.276)*
Figure 2-11 Example of the formation of an external retains resulting from casting a wall onto a previously hardened slab (Ballim & Graham, 2009, p.274)22
Figure 2-12 Formation of stresses within a large concrete element induced by internal
restraints caused by a non-uniform distribution of temperature (Ballim & Graham, 2009,
p.275)
Figure 2-13 Typical Semi-Adiabatic calorimeter (Cost, 2008)
Figure 2-14 Example of semi-adiabatic and fully-adiabatic temperature profiles (Weakley,
2010)
Figure 2-15 Thermal profile of a Portland cement paste where the inter sample temperature
has been subtracted (ASTM draft, 2012)28
Figure 2-16 Signal and noise determination for verification of minimum ratio (ASTM draft,
2012)30
Figure 2-17 Setting time mark shown at 20% and 50% fractions of the main peak response
temperature rise of a typical concrete mixture (ASTM draft, 2012)31
Figure 2-18 Schematic of adiabatic calorimeter arrangement (Ballim & Graham, 2005, p.12)
32
Figure 2-19 Local Portland cement heat curves (Ballim & Graham, 2009, p.278)33
Figure 2-20 The heat curves of Figure 2-14 expressed in maturity form (Ballim & Graham,
2009, p.279; Grieve, 2009; Grieve, 2009)
Figure 2-21 Typical manual Vicat apparatus for determination of standard consistence and
setting time
Figure 3-1 Semi-adiabatic calorimeter insulation
Figure 3-2 Experimental setup of semi-adiabatic calorimeter
Figure 3-3 DAQ system configuration diagram (National Instruments , 1996, p.2)41
Figure 4-1 Effects of varied insulation and sample mass on repeated paste mixtures (ASTM
draft, 2012, p.25)*45
Figure 4-2 Temperature profiles of experimental mixtures and the corresponding inert
profiles46
Figure 4-3 Heat profiles for experimental mixtures
Figure 4-4 Heat profile comparison between CEM I 42.5N and CEM I 52.5N with slag
addition, measured by fully adiabatic calorimetry and semi-adiabatic calorimetry
respectively*
Figure 4-5 Heat rate profiles of experimental mixtures
Figure 4-6 Profile comparison between CEM I 42.5N and CEM I 52.5N with slag addition
(GGBS and GGCS), measured by fully adiabatic calorimetry and semi-adiabatic calorimetry
respectively*52
Figure 4-7 Temperature profiles of experimental mixtures with setting time makers shown at
initial and final setting times*54
Figure 4-8 Heat rate profiles of experimental mixtures with setting time makers shown at
initial and final setting times56

### VIII

## List of equations

Equation 2-1 Tricalcium silicate hydration	7
Equation 2-2 Dicalcium silicate hydration	
Equation 2-3 Pozzolanic reaction	7
Equation 2-4 Fourier equation (two dimensional form)	31
Equation 2-5 Heat evolved at any time per unit mass of binder	33
Equation 2-6 Rate of heat evolved	33
Equation 2-7 Extent of maturity of concrete	34
Equation 2-8 Heat rate derived from maturity rate	34

#### 1 Introduction

#### 1.1 Background and context

A new slag extender was introduced into the Western Cape market in 1999 under the name of ground granulated Corex slag (GGCS), and was been found to have a higher reactivity than ordinary blastfurnace slag (GGBS), when supplemented with Portland cement (PC). The higher reactivity has led to the production of superior concretes, with improvements in both strength and durability. However coupled with these improvements are other characteristic changes that need to be investigated to ensure effective placement of GGCS concrete. The characteristics that are of focus in this dissertation are the thermal profiles that develop during the hydration of GGCS concrete and how it translated to the evolution of heat as well as the setting time of the concrete.

The reaction between water and cement is a complex exothermic reaction and the heat produced due to this reaction is commonly known as the heat of hydration. The temperature of all concrete constituents is raised due to the heat of hydration, and therefore in order to determine the thermal properties of the composite all the individual components need to be considered. The heat liberated during the reaction is of interest due the potential formation of thermally induced cracks resulting from temperature differentials that form stresses during the hardening of early-age concrete. Apart from the formation of thermal cracks, the heat of hydration is also of interest with regard to the time of set and strength development over time, as the heat of hydration is directly related to the chemical reactions that take place within concrete to develop its rigid structure over the curing period.

The analysis of temperature and stress development is an extremely non-linear problem due to the dynamic nature of the hydration process, which is both highly time and temperature dependent. Modelling the generation and transfer of heat within concrete is vital to predicting the behaviour of concrete at early-ages, especially with regard to the placement of large concrete elements.

#### 1.2 Problem statement

South African cementitious materials need to comply with standards specified by SANS 50197-1, but the standards permit varying combinations of composition (see Table 2-4 on page 10). Cement Manufacturers have the liberty to produce cements within the specified constrains, that are technically feasible and economically viable. This results in varying compositions of cements, under the same type (e.g. CEM II A-S), being produced by different manufactures. With the introduction of Corex slags into the market it is important to differentiate this slag from GGBS and clearly identify the fundamental characteristic variation as different cement manufacturers incorporate the slag. Once these characteristic are clearly determined it is vital that the relevant industries are made aware to prevent unexpected variations of concrete design mixes, such as high heat evolution and extended setting time, which may result in thermal cracking and induced time constraint respectively.

Slags in general reduce the rate of heat generated by concrete and decrease the setting time, but from the reviewed literature (see section 2.2) the Corex technology of iron production has

been found to produce slag of a slightly different chemical composition resulting in varied effects on the heat liberated during concrete curing and setting time. Alexander et al. (2003) found that GGCS concretes do not produce the heat reduction advantage that GGBS concretes do, and further stated that no appreciable difference was found when compared to the heat of hydration of PC (CEM I 42.5).

#### 1.3 Objectives

The goals of this dissertation are to develop an understanding of the hydration reaction that takes place in the formation of concrete and how the heat liberated may affect the structural properties of early-age concrete elements. Different methods of measuring the heat of hydration, through means of calorimetry, will be reviewed as well as how the results obtained from these methods are used to model temperature profiles within concrete elements.

Ultimately the thermal profiles of three different cement paste mixtures are experimentally measured by means of semi-adaibatic calorimetry to compare the heat liberated. The cement pastes are differentiated by the binder composition. All three sample will contain commercially available PC (CEM I 52.5 N), with sample 1 being 100% PC. Sample 2 and 3 with be blended with 50% GGCS and 50% GGBS respectively, which will allow a comparison to be made between the two slags.

Further, an investigation is made into the relationship between the main peak response (MPR) of the temperature profile developed by the cement paste and the associated setting times. This relationship was put forward in a draft standard developed by ASTM (2012) and an attempt is made to validate this relationship against SANS 50196-3 (2006).

#### 1.4 Justification of study

The cement industry is large and well established within South Africa and with the introduction of the government's National Development Plan, with a focus on 'critical' infrastructure, cement demand is likely to rise. The rise in demand could result in variations of cement composition as resources are more broadly sourced and imports expanded. It is for these reasons that regular testing and regulation pertaining to cement composition needs to be encourage.

This report focuses on the thermal behaviour of GGCS and how it differs from regular blastfurnance slag. This is of importance in providing the correct thermal properties required to prevent thermal cracking with the use of temperature prediction models. The thermal properties of GGCS and GGBS concretes were compared by Alexander et al. (2003) but a lower strength class PC was used (CEM I 42.5), therefore further evaluation of the slags using CEM I 52.5 may be useful.

Comparing the thermal profiles developed by the cement pastes to the corresponding setting time will shed light on potential relationship, which if validated may be used as a means of quality control by concrete manufacturers and contractors.

Ultimately any research into the use of the relatively new Corex slag may be useful to the construction industry globally as more countries worldwide adopt the Corex process of

producing iron, which will render Corex slags available to them. Currently the Corex method of iron production has only been implemented in three countries South Africa, India and China (Siemens VAI, 2013), but it is unclear whether the slags produced are being utilised in the concrete industry outside South Africa.

#### 1.5 Scope and limitations

The thermal profiles developed are limited to cement pastes because the standard method for evaluating setting time (SANS, 2006) only makes use of paste in determining standard specifications of cements and not concrete. Due to time constrains and availability of equipment the conclusions made are based on a relatively small data sets and therefore further testing is needed for validation.

The custom build semi-adiabatic calorimeter used in experimentation was constructed from polystyrene to insulate the test samples. An alternate insulation material with a lower thermal conductivity may be better suited as less heat will be lost to the environment, therefore based on the scope of the assessment conducted only relative comparisons can be made.

Temperature measurement were carried out with thermocouples, which are a convenient, robust and relatively cheap sensors, but other sensors such as thermistors and resistance temperature detectors (RTD) have a greater accuracy and are more responsive to temperature variations. Although robust thermocouples are well suited to cement/concrete thermal measurement, more fragile sensors should be considered for more accurate hydration heat determination.

#### 1.6 Outline of dissertation

This dissertation proceeds with a literature review of relevant topics associated with the experimental procedure, essentially acting as a point of reference. A description of the experimental procedures, which follows the literature review, describes and justifies the experimental methods chosen by drawing on the literature reviewed. The results are then presented and discussed in the proceeding section. Finally conclusions are made based on the main findings from the results obtained and again reference is made to the literature.

#### 2 Literature Review

This literature review covers the fundamentals of cementitious materials and concrete, with particular attention being paid to slag extenders and the associated production technologies (Corex and blastfurnace). Focus is then shifted towards the thermal properties of concrete and the calorimetric methods used to measure the heat liberated during the hydration of cementitious materials. Finally two methods of determining setting time are reviewed. The aim of the literature review is to clarify the direction taken in the experimental program conducted.

#### 2.1 Cementitious materials

Cement forms a matrix within hardened concrete and mortar. When this matrix forms it acts as a binding agent to produce a strong rigid composite when combined with varying grades of aggregate. Portland cement is the most widely used cement in the construction industry and is often combined with cement extenders. Different combinations of cement and extender blends produce composites of varying properties. Extenders are defined as materials that provide cementing properties when in combination with Portland cement.

#### 2.1.1 Portland cement

Portland cement is the most commonly used base of cementitous materials due to the following:

- It is relatively cheap to produce
- Setting and hardening take place at normal temperature and pressure
- Setting and hardening can take place under water
- Strong and durable concrete can be formed

The primary raw materials of Portland cement (PC) are oxides of calcium, silica, aluminium and iron. The table below gives a brief breakdown of the different oxides; as well as how they are obtained and function they form.

Material Oxide		Symbol	Obtained	Function
Lime	Calcium oxide	CaO	Heating Limestone	Cementing compounds
Silica	Silicon dioxide	$SiO_2$	Clay and Shale	Cementing compounds
Alumina	Aluminium oxide	$Al_2O_3$	Clay and Shale	Fluxing agent
Iron	Ferric oxide	Fe <sub>2</sub> O <sub>3</sub>	Clay and Shale	Fluxing agent

Table 2-1 Primary raw materials of PC (Owens, 2012)

#### 2.1.2 Manufacturing process

Upon entering a kiln, Calcium carbonate (limestone or calcite) is converted to calcium oxide  $(CaCO_3 \rightarrow CaO + CO_2)$  at a temperature between 800 and 1000°C. The blend of oxides is when further heated to approximately 1450°C to form the cement clinker. The clinker also contains magnesia and alkalis as well as the ash from the fuel used in the kiln, but between 63% and 69% of the clinker is CaO (Fulton, 2012). There are four dominant compounds

present in the cement clinker, tricalcium silicate, dicalcium silicate, tricalcium aluminate and tetracalcium aluminoferrite. The addition of Gypsum at the milling stage provides a retarding agent for the rate of hydration of cement. Portland cement contains a large proportion on tricalcium silicate, which distinguishes PC from other lime and silica based cements. Table 2-2 shows the compound breakdown of a common South African cement (CEM I)

Table 2-2 Primary raw materials of PC (Fulton, 2012, p.22)

Compound	mpound Formula Al		% by mass in cement
Tricalcium silicate	3CaO.SiO <sub>2</sub>	$C_3S$	60 – 73
Dicalcium silicate	2CaO.SiO <sub>2</sub>	$C_2S$	8 - 30
Tricalcium aluminate	3CaO.Al <sub>2</sub> O <sub>3</sub>	C <sub>3</sub> A	5 - 12
Tetracalcium aluminoferrite	4CaO.Al <sub>2</sub> O <sub>3</sub> .Fe <sub>2</sub> O <sub>3</sub>	$C_4AF$	8 - 16
Magnesia	MgO	M	1,9 - 3,2
Gypsum	Raw material	-	4,4 – 6,7
Free lime	CaO	-	0,2-2,5

#### 2.1.3 Cement Extenders

Cement extenders are defined as materials that have cementing properties when in combination with PC. Extenders are by-products derived from iron making, electricity generation and silicon smelting processes and therefore are economically viable substitutes for PC. Cement extenders can also offer technical advantages in the formation of concrete.

The following are example of extenders used within the concrete industry:

- Ground granulated blastfurnace slag (GGBS)
- Ground granulated Corex slag (GGCS)
- Fly ash (FA)
- Condensed silica fume (CSF)

**GGBS** is a bi-product of the blastfurnace processes in the production of iron and consists mainly of alumina and silica.

**GGCS** is a bi-product of the Corex processes in the production of iron (see section 2.2)

**FA** is produced through extraction by electrostatic precipitators or bag filters from flue gases of furnaces fuelled by pulverised coal.

**CSF** is a by-product of the ferrosilicon smelting process. Vapour from the process is condensed to form CSF.

Table 2-3 on the following page shows the effects of these extenders on the properties of concrete.

Table 2-3 Effects of extenders on concrete properties (Grieve, 2009, p.4)

Extender	Effects	Suitability for use in:						
		Mass concrete pours	Shotcrete	Chloride exposure	Sulphate exposure	ASR conditions		
GGBS	Fresh concrete  -May improve workability slightly -Retards setting slightly Hardened concrete -Slows development of strength -Increases later age strength, eg at 90 days -Refines pore structure and reduces permeability -Increases rate of carbonation -Prevents or retards alkali-silica reaction -Binds chlorides and reduces the chloride induced corrosion of embedded steel -Reduces rate of heat generation caused by cementing reactions.	High GGBS contents (>50%) help reduce the risk of thermal cracking	No particular benefit	GGBS is particularly suited to chloride capture and provides significant enhancement of resistance to chloride attack of reinforcement	Get specialist advice based on latest research findings from C&CI	Requires >40% GGBS content to control potential ASR for sensitive aggregate types		
FA	Fresh concrete -Improves workability and reduces water requirement for a given slump -Slightly retards setting. Hardened concrete -Slightly reduces rate of strength developmentIncreases later age strength, e.g. at 90 days -Reduces the rate of chloride diffusion through concreteRefines pore structure and reduces permeabilityPrevents or retards alkali-silica reaction -Improves sulphate resistance -Reduces rate of heat generation caused by cementing reactions.	FA content of 30% or more will significantly reduce the risk of thermal cracking	Increased paste content should improve adhesion	FA content of 30% or more will enhance resistance to chloride attack of reinforcement	FA content of 30% or more should improve the sulphate resistance of concrete	Requires FA content of >20% to control potential ASR for sensitive aggregate types		
CSF	Fresh concrete -Reduces workability -Increases cohesiveness -Reduces bleeding significantly. Hardened concrete -Increases strength -Reduces permeability.	Not suitable	CSF is particularly suited to reducing rebound in shotcrete applications	Use of CSF has potential to significantly reduce permeability and improve resistance to chloride ingress	Use of CSF has potential to significantly reduce permeability and reduce susceptibility for sulphate ingress	Requires CSF content of >15% to control potential ASR for sensitive aggregate types		

#### 2.1.4 Hydration

The reaction between the PC and water is referred to as the hydration of PC. The four main compounds, tricalcium silicate  $(C_3S)$ , dicalcium silicate  $(C_2S)$ , tricalcium aluminate  $(C_3A)$  and tetracalcium aluminoferrite  $(C_4AF)$  all take place in reactions to form hardened cement paste. The most important of these reactions involves  $C_3S$  and  $C_2S$  in the formation of calcium silicate hydrate  $(C_3S_2H_3)$ . The chemical equations for tricalcium silicate hydration and dicalcium silicate hydration can be seen below.

$$C_3S + 6H \rightarrow C_3S_2H_3 + 3Ca(OH)_2$$
 (2-1)

$$C_2S + 4H \rightarrow C_3S_2H_3 + Ca(OH)_2$$
 (2-2)

(\*Note H represents H<sub>2</sub>O)

Most of the strength in hardened cement paste is provided by the formation of calcium silicate hydrate (also represented by C-S-H). C-S-H forms at the surface of particles of unhydrated cement and grows outward in a rigid structure know as gel, which is represented graphically in Figure 2-1 on the following page. The gel comprises of minute rods and platelets connected at contact points. Calcium hydroxide, Ca(OH)<sub>2</sub> forms comparatively large crystals which are embedded within the C-S-H gel. Ca(OH)<sub>2</sub> does not provide any structural strength but does raise the pH of the pore water to approximately 12.5 (Fulton, 2012), as some Ca(OH)<sub>2</sub> is found in solution. The high alkalinity provides corrosion resistance for embedded steel reinforcing.

Ca(OH)<sub>2</sub> is also available to react with **pozzolans** such as FA and CSF. In a pozzolanic reaction calcium hydroxide is consumed to form C-S-H gel and therefore further strength is produced from the introduction of pozzolan extenders. This reaction was utilised in Roman concrete produced in ancient Rome to build structures such as the Pantheon (Lechtman & Hobbs, 1986). At the basis of this reaction is a simple acid-base reaction between calcium hydroxide and silicic acid (H<sub>4</sub>SiO<sub>4</sub> or Si(OH)<sub>4</sub>). The reaction in its abbreviated notation is below.

$$CH + SH \rightarrow C_3 S_2 H_3 \tag{2-3}$$

The high pH environment also enables GGBS and GGCS to hydrate and form C-S-H gel, but in this case calcium hydroxide is not produced and GGBS and GGSC are said to have **latent hydraulic** properties.

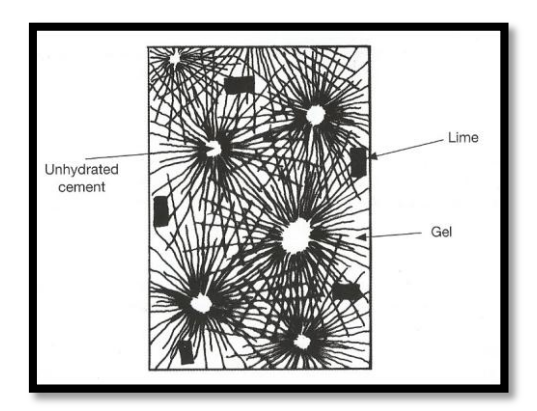


Figure 2-1 Structure of hardened concrete paste (Grieve, 2009)

#### 2.1.5 Heat liberation through hydration of cement

Ballim and Graham reference Roy (1989) in describing the hydration process, in which three stages of the hydration reaction are developed and represented on the curve in Figure 2-2 below. The curve shows the development of the heat of hydration with respect to time in stages. Stage 1 begins immediately after water is added and the hydration reaction commences with an initial peak. This peak is said to be primarily due to C<sub>3</sub>A hydration as opposed to C<sub>2</sub>S. The hydration of C<sub>3</sub>A is retarded due to the formation of ettringite which forms a partially protective barrier to the reaction, resulting in a rapid decrease in heat rate. From this point the liberation of heat continues at a low rate and is mainly due to the hydration of C<sub>3</sub>S to form CSH (Calcium Silicate Hydrate). The second stage is characterised by a well-defined second peak due to a rapid increase in the rate of heat liberation followed by deceleration, as the hydrates C-S-H and Ca(OH)<sub>2</sub> are formed. Setting occurs near this inflection point which is indicative of sufficient C-S-H formation to produce a rigid network structure. A third minor peak, referred to as a shoulder, often occurs due to the transformation of ettringite to monsulphate hydrate form.

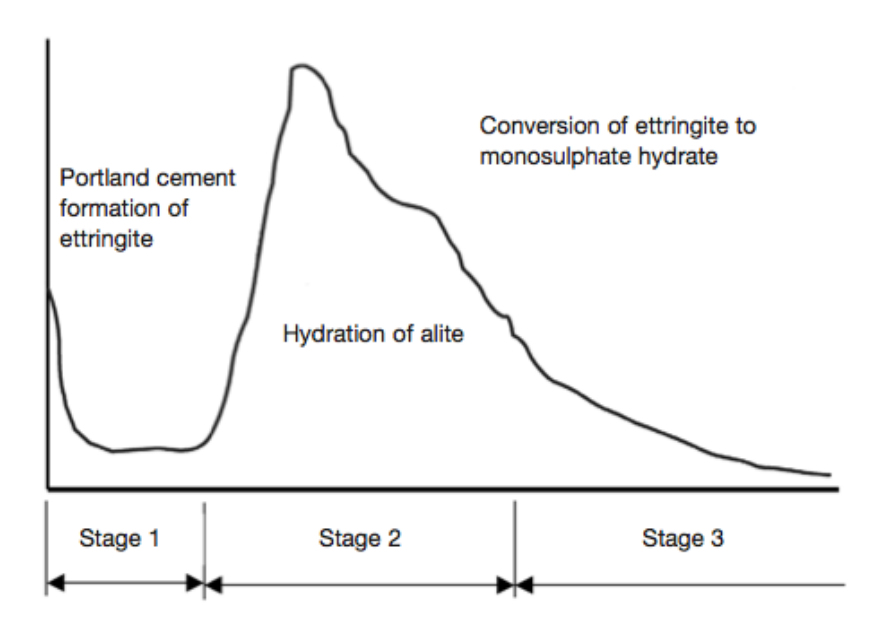


Figure 2-2 Classification stages of hydration developed by isothermal calorimetry (Roy, 1989)

#### 2.1.6 Setting and hardening of concrete

Once water is added to the cement, extender and aggregate blend the hydration reaction begins and the concrete stiffens gradually over time. The hydration reaction is exothermic and typical PC has a heat of hydration of approximately 375 J/g (Fulton, 2012), which elevates the temperature of fresh concrete as its sets and becomes unworkable. A sufficient ratio of water to cement is required to provide adequate plasticity when working with concrete.

The rate of hydration is not uniform. The reaction is rapid as water is mixed with cement, dissolving the cement particles and allowing the hydration of tricalcium silicate to form C-S-H gel. At this stage the mixing water becomes supersaturated with calcium hydroxide. The reaction slows as calcium sulphoaluminate (ettringite) precipitates due to the reaction of dissolved aluminates and gypsum. It is assumed that the ettringite attaches itself to the aluminte, preventing its access to water, thus providing a retarding effect. This effect is reduced over time as further reactions take place.

This process is divided into three stages (Fulton, 2012), which are as follows:

- Dormant stage the paste remains plastic and workable
- Setting stage the paste becomes stiff and unworkable
- Hardening stage the paste is in a rigid solid stage and strengthens over time

The transition between the first two stages is referred to as the *initial set* and the transition between the last two stages is referred to as the *final set* (Refer to Figure 2-2 on Page 8)

#### **2.1.7** Curing

Water-filled space is required for the formation of cementing compounds in cement paste. This is the case for both hydration reactions (PC, GGBS & GGCS) and pozzolanic reactions (FA & CSF). These reactions are also dependent on temperature. The rate of reaction increases with increasing temperature and can drop to zero at extremely low temperatures.

Temperature and moisture maintenance are therefore vital in ensuring that continual rates of hydration and pozzolanic reactions. This process is defined as curing and relates directly to strength development of concrete as well as the development of impermeability of the near surface of concrete. Therefore curing is a particularly important factor in producing durable concrete.

#### 2.1.8 Common cements

The following are the standards for "common cements" in South Africa

- SANS 50197-1 Cement Part 1: Composition, specification and conformity criteria for common cements
- SANS 50197-2 Cements Part 2 Conformity evaluation

There are 27 "common cements" covered in the standard, all comprising different proportions of constituents. The products are grouped into 5 main cement types, CEM I to CEM V. SANS 50197-1 provides a detailed breakdown of the permitted products, which can be seen in the table below.

			Composition, percentage by mass <sup>(a)</sup>										
Main types	Notation of (types of c ceme	ommon	Clinker	Blast- furnace slag		Pozze		Fly	ash Calca-	Burnt shale	Lime	stone	Minor additio- nal constit-
			K	S	$D^{(b)}$	P	Q	V	w	T	L	LL	uents
CEM I	Portland cement	CEM I	95 - 100	-	-	-	-	-	-	-	-	-	0 - 5
	Portland-slag	CEM II A-S	80 - 94	6 - 20	-	-	-	-	-	-	-	-	0 - 5
	cement	CEM II B-S	65 - 79	21 - 35	-	-	-	-	-	-	-	-	0 - 5
	Portland-silica fume cement	CEM II A-D	90 - 94	-	6 - 10	-	-	-	-		-	-	0 - 5
		CEM II A-P	80 - 94	-	-	6 - 20	-	-	-	-	-	-	0 - 5
	Portland- pozzolana	CEM II B-P	65 - 79	-	-	21 - 35	-	-	-	-	-	-	0 - 5
	cement	CEM II A-Q	80 - 94	-	-	-	6 - 20	-	-	-	-	-	0 - 5
		CEM II B-Q	65 - 79	-	-	-	21 - 35	-	-	-	-	-	0 - 5
	Portland-fly ash cement	CEM II A-V	80 - 94	-	-	-	-	6 - 20	-	-	-	-	0 - 5
		CEM II B-V	65 - 79	-	-	-	-	21 - 35	-	-	-	-	0-5
CEM II		CEM II A-W	80 - 94	-	-	-	-	-	6 - 20	-	-	-	0 - 5
		CEM II B-W	65 - 79	-	-	-	-	-	21 - 35	-	-	-	0 - 5
	Portland-burnt	CEM II A-T	80 - 94	-	-	-	-	-	-	6 - 20	-	-	0 - 5
	shale cement	CEM II B-T	65 - 79	-	-	-	-	-	-	21 - 35	-	-	0 - 5
		CEM II A-L	80 - 94	-	-	-	-	-	-	-	6 - 20	-	0 - 5
	Portland- limestone	CEM II B-L	65 - 79	-	-	-	-	-	-	-	21 - 35	-	0 - 5
	cement	CEM II A-LL	80 - 94	-	-	-	-	-	-	-	-	6-20	0 - 5
		CEM II B-LL	65 - 79	-	-	-	-	-	-	-	-	21 - 35	0 - 5
	Portland-	CEM II A-M	80 - 94	-				6 - 20				<b>→</b>	0 - 5
	composite cement <sup>(c)</sup>	CEM II B-M	65 - 79	-				21 - 35				<b>→</b>	0 - 5
		CEM III A	35 - 64	36 - 65	-	-	-	-	-	-	-	-	0 - 5
CEM III	Blastfurnace cement	CEM III B	20 - 34	66 - 80	-	-	-	-	-	-	-	-	0 - 5
	Comon	CEM III C	5 - 19	81 - 95	-	-	-	-	-	-	-	-	0 - 5
	Pozzolanic	CEM IV A	65 - 89	-	<b>←</b>		11 - 35	_	<b>→</b>				0 - 5
CEM IV	cement <sup>(c)</sup>	CEM IV B	45 - 64	-	←		36 - 55		$\longrightarrow$		-		0 - 5
	Composite	CEM V A	40 - 64	18 - 30	-	-	18 - 30	<b>→</b>			-	-	0 - 5
CEM V	cement <sup>(c)</sup>	CEM V B	20 - 39	31 - 50		←	31 - 50	$\longrightarrow$	-	-	-		0 - 5
Notes													

- (a) The values in the table refer to the sum of the main and minor additional constituents.
- (b) The proportion of silica fume is limited to 10%.
- (c) In portland-composite cements CEM II A-M and CEM II B-M, in pozzolanic cements CEM IV A and CEM IV B, and in composite cements CEM V A and CEM V B, the main constituents other than clinker shall be declared by designation of the cement.

Table 2-4 Permitted products in SANS 50197-1 (Owens, 2012, p.29)

#### **Cement for concrete**

Common cements (CEM I to V) produced in factories or onsite blends of common cements and extenders may be used in concrete. Blended cements can lead to per unit mass cost reductions, but may require a higher skill level on site in order to ensure good quality curing practices are adhered to.

#### 2.1.10 Water:cement ratio (W/C)

The ratio of the mass of water to the mass of cement is defined as the water:cement ratio, where the mass of cement comprises of all cementitious material (PC and extenders). Strength and permeability of cement paste are highly dependent on the W/C ratio at any degree of hydration or pozzolanic reaction. Therefore the W/C ratio is a key design property as it is a vital indicator of the strength and impermeability of hardened concrete. Strength increases and permeability decreases as the W/C ratio is reduced, ranging from 0.25 for high performance concrete, to 1.15 for cement plaster (Fulton, 2012, p.37). The figure below displays the affect the W/C ratio on the compressive strength of different design mixtures.

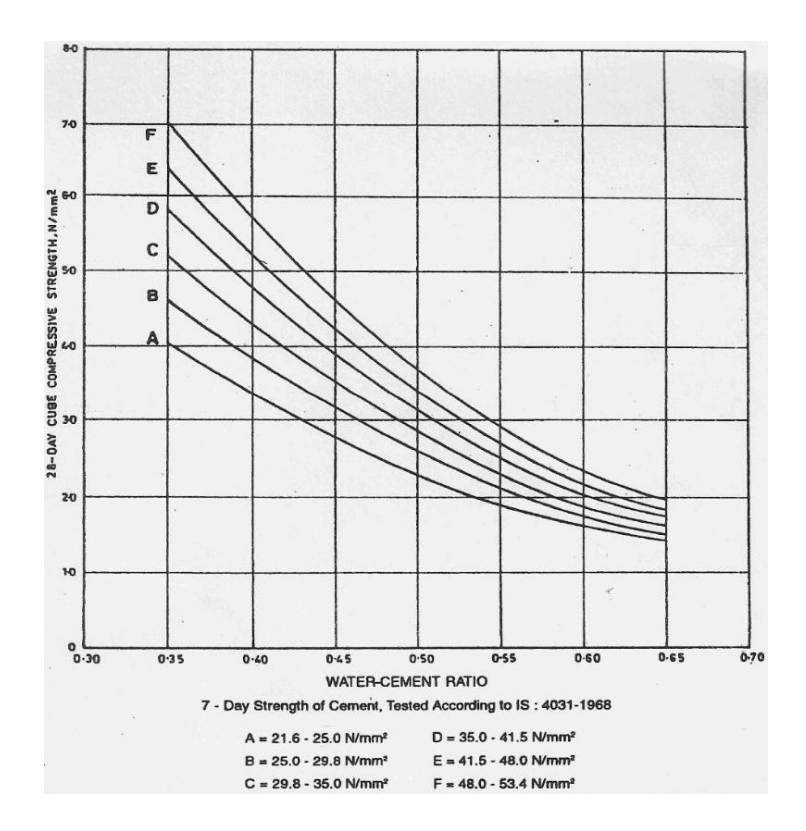


Figure 2-3 Relationship between water:cement ratio and concrete compressive strength for different cement strengths using crushed aggregate (Kishore, 2010)

#### 2.1.11 Conclusion

PC is the most widely used cement in the construction industry and extenders provide cementing properties only in conjunction with PC, which is the most reactive of the cementitious materials. Pozzolans are reliant on the calcium hydroxide that forms through the hydraytion of PC, to form C-S-H and therefore adds to the strength development. The high pH environment also enables slags to hydrate, which are said to have latent hydraulic properties. The heat liberated through the hydration of cement is broken up into stages where two defined peaks are formed. The second larger peak is associated with a rapid increase in the rate of hydration and setting occurs near the inflection point of this peak. The hydration and pozzolanic reactions are both temperature dependent, increasing as temperature rises, therefore temperature management is vital in the curing process.

#### 2.2 Corex and blastfurnace slags

The slags GGCS and GGBS are bi-products of the iron processing industry and are both utilised as cement extenders. The difference between the two slags is in the manufacturing technology of the iron production, which results in the slags having different compositions. Extensive research into Corex slags has been conducted and shown GGCS to have superior characteristics to existing blastfurnace slags extenders (Alexander et al., 2003). Although very little literature is available on Corex slags as extenders. This could be attributed towards the limited availability and use of the Corex slags globally. Saldanha Steelworks is the only plant in South Africa producing commercially available GGCS extender (Grieve, 2009). From the research conducted by Alexander et al (2003) it was believed that the introduction of GGCS in to the Western Cape, since October 1999, had had a significant impact on the durability and economy of the concrete structures within the region. A summary of the findings of this research follows.

#### 2.2.1 Slag characterisation

Slag constituents are derived from iron oxide ore and lime, and mainly consist of silica and alumina. The slag forms a glassy material when rapidly cooled by means of water quenching. As mentioned in section 2.1.4 slags are latent hydraulic binder and are essentially fuelled by the hydration of Portland cement, but slag performance is dependent upon the material chemistry, glass content and how finely the slag is ground.

An Oxide analysis of PC, GGBS and GGCS is presented in Table 2-5 below. From this analysis it can be seen that GGCS has higher concentrations of CaO, Al<sub>2</sub>O and MgO but lower SiO<sub>2</sub>, which is indicative of higher hydraulic activity when comparisons were done on GGBS and GGCS of equivalent fineness, using the most accepted hydraulic activity formulae (Mantel, 1994)

T 11 A F	$\Delta$ 1 1 .	e Da	CODO 1	$\alpha$	0/1	/T C 11	2002)
Table 7-5	Oxide analysis	AT PL	(-(-KS and	1-1-1	Va hy macc	/ lauteerally	700071
	Oniuc amarysis	VI I C.	OODS and	$uuv_{0}$	/ U D Y 111433	\Jaulttan \.	40041

Oxides	PC	GGBS	GGCS
CaO	67.2	34.0	37.2
SiO <sub>2</sub>	22.3	35.5	30.8
$Al_2O_3$	4.4	15.4	16.0
MgO	1.01	9.4	13.7
TiO <sub>2</sub>	0.22	1.2	0.51
Fe <sub>2</sub> O <sub>3</sub>	3.4	0.98	0.87
MnO	0.08	0.88	0.09
K <sub>2</sub> O	0.56	0.87	0.35
Na <sub>2</sub> O	0.21	0.16	0.12
SO <sub>3</sub>	0.58	2.49	3.19

Physical properties also affect slag reactivity; in particular a higher fineness will result in a more reactive material. Surface area comparisons of PC, GGBS and GGCS can be seen in Table 2-6 below, where results using both the Blaine and BET fineness method are shown. The results reveal that GGCS is clearly a finer material then both PC and GGBS. GGCS was also shown to have a higher proportion of ultra-fine particles ranging from 1-10 microns, which leads more cohesive concretes.

Table 2-6 Physical	properties of PC,	<b>GGBS</b> and <b>GGCS</b>	(Alexander et al.,	2003, p.9)

Method	PC	GGBS	GGCS
BET fineness (m²/kg)	-	991	1145
Blaine Fineness (m²/kg)	310	390	467
% passing 1 micron	-	6	7
% passing 10 micron	-	45	51

#### 2.2.2 Corex slag concrete

Replacement levels of slag generally vary between 30 to 70%, with 50% being the optimum level based on compressive strength, but construction constrains and technical material properties also need to be considered. Furthermore replacement level were found to be directly related to desired age based strength as well as w/b ratios, with GGCS concretes displaying higher strength at early age when that of similar GGBS based concretes. These findings are clearly illustrated in Figure 2-4 below.

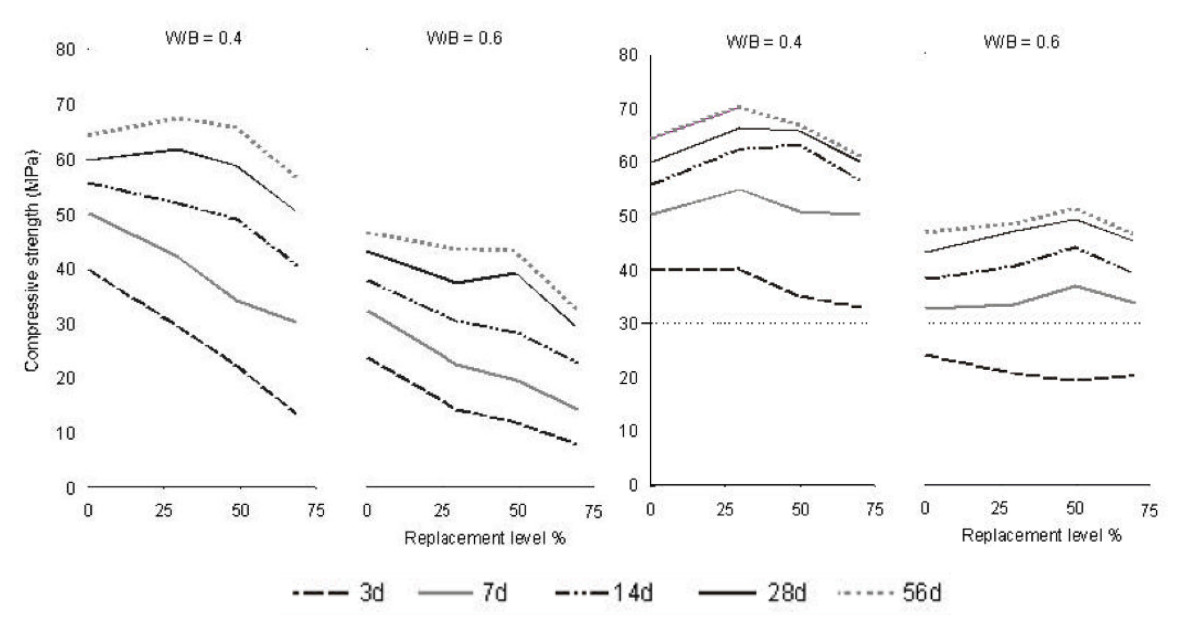


Figure 2-4 Compressive strength of GGBS (left) and GGCS (right) as functions of slag replacement and w/b ratio (Alexander et al., 2003, pp.12-13)

Alexander et al. (2003) found that Corex slags reduce the amount of binder required to produce concrete with a characteristic strength of 30 MPa made with Western Cape aggregates. This reveals a clear economic advantage to using Corex slags as well as a

potential reduction in environmental impact due less industrially intensive products being required in concrete based construction.

#### 2.2.3 Fresh and hardening properties of Corex slag based concrete

**Workability** may be improved with the introduction of slags to the cement paste, which is attributed to better particle dispersion and lubrication that results from finer slag grains. In terms of water demand slags offer little reduction due to the angular nature of the particles and in the case of GGCS concrete water demands were found to be similar to 100% PC concretes. (Alexander et al., 2003)

**Setting times** are found to increase with the introduction of GGCS to PC, this is because slags are latent hydraulic binder and react slower with water than PC. The increase in setting time is important factor for contractors as the time to finish an operation may be delayed by as much as two hours, but the obvious advantage is that more time can be allocated to placement and compaction. Alexander et al. (2003) calculated initial and final setting times of PC and GGCS concretes (See Table 2-7) by SABS method 196-3 (1994), but no comparison was made with GGBS.

In terms of **bleeding** slag concretes in general are found to have lower rates which are attributed to the finer slag particles holding water in the mix, which is coupled with increased cohesion in the paste, therefore reducing segregation. However slag concretes bleed for longer periods due to the increased time to set. This relationship with Corex slags can be seen for w/b ratios of 0.4 and 0.6 in Figure 2-5.

Table 2-7 Intial and final setting time for standard cementitious pastes (Alexander et al., 2003, p.14)

Property	100% PC	30% GGCS	50% GGCS	70% GGCS
Initial set (min)	170	240	270	265
Final set (min)	255	325	355	420

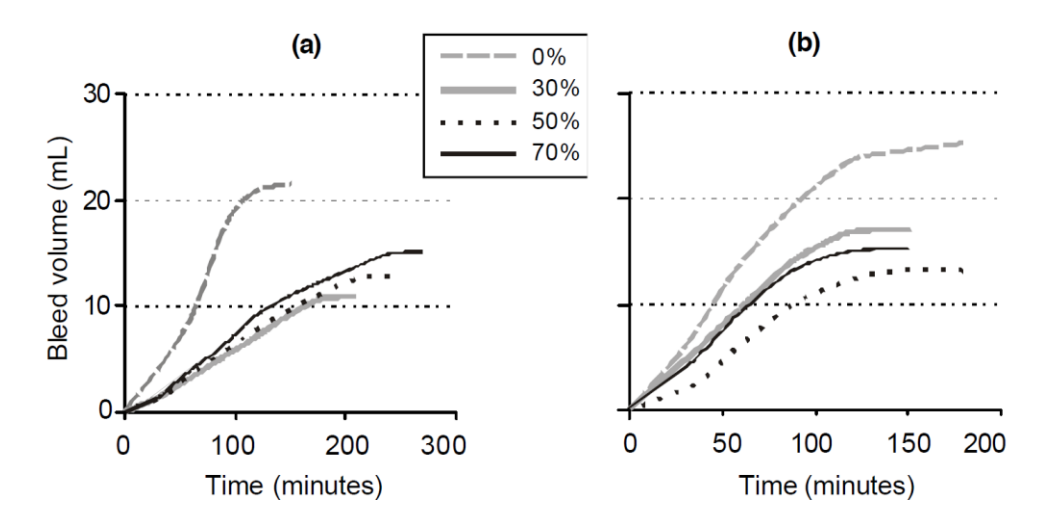


Figure 2-5 Bleeding characteristics of concrete for varying Corex slag contents, with (a) w/b = 0.4 and (b) w/b = 0.6 (Alexander et al., 2003, p.15)

Slag concretes are less likely to incur **plastic settlement cracking** as a result of decreased bleeding, but in the case of **plastic shrinkage cracking** all concretes are at risk under hot windy conditions. It is therefore vital to ensure that the evaporation rates do not exceed bleeding rates as plastic shrinkage may occur before the concrete has developed sufficient stiffness. The reduced bleeding rates and increased time of setting of slags need to be considered as the risk of plastic shrinkage, which may result in early-age cracking, is increased. Measures such as plastic covering, fog spraying or sheltering of concrete should be implemented in conditions where the evaporation rates are in excess of 1.0 kg/m²/hr (Alexander et al., 2003).

#### 2.2.4 Heat of hydration

An advantage of GGBS based concretes is the reduced rate of heat development during hydration when supplemented with PC concretes. This characteristic has the benefit of reducing the risk of **thermal cracking** (see section 2.3.2). However, the higher reactivity of GGCS concretes result in no appreciable reduction in the heat generated during hydration when compared to concretes produced with 100% PC. On the other hand, for concretes of equivalent compressive strength the reduction of the required binder content resulting from GGCS replacement will reduce the heat of hydration and decrease the risk of thermal cracking. Figure 2-6 shows the total heat plots of PC, GGBS and GGCS concretes calculated be means of **adiabatic calorimetry** (see section 2.4).

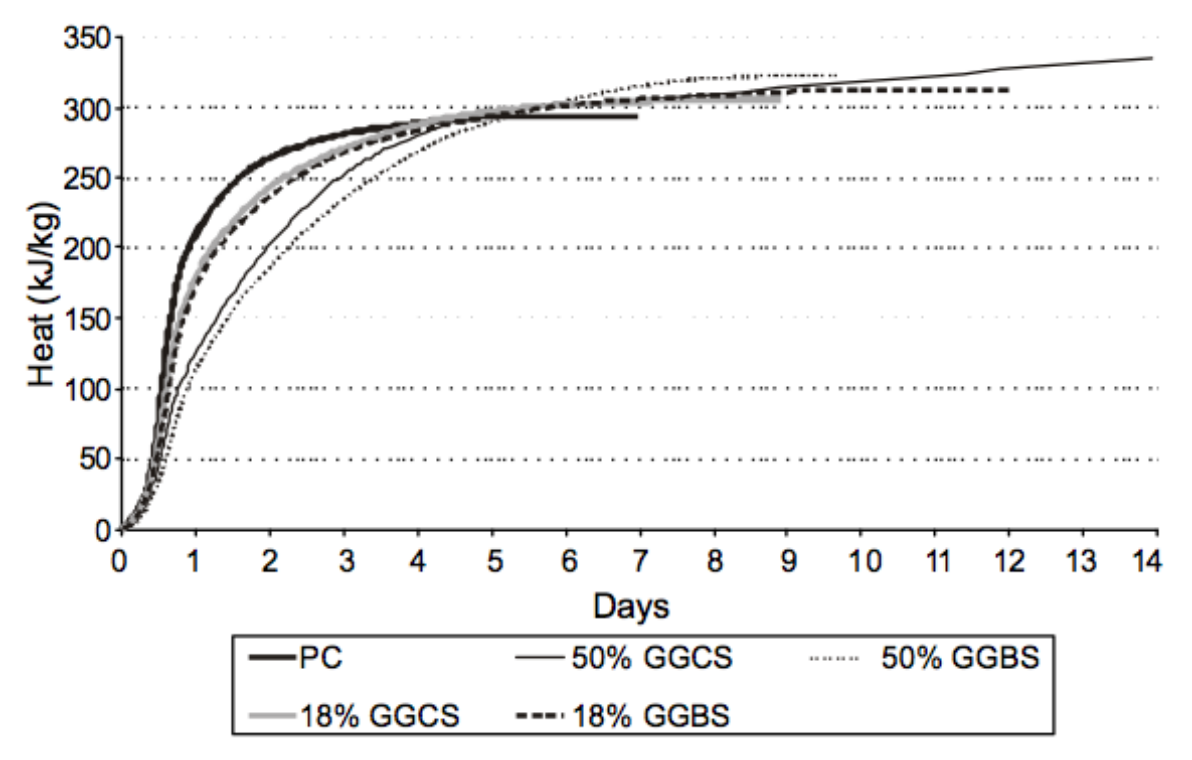


Figure 2-6 Total heat produced during hydration for different slag binder combinations (Alexander et al., 2003, p.17)

#### 2.2.5 Durability of slags

Transport processes such as absorption, permeation and diffusion are key factors in calculating the deterioration potential of concrete. Indexes, to measure these factors, have been developed through research geared towards improving the durability of concrete structures in South Africa. From this research an index testing manual was been compiled (Alexander et al., 1999). It is important to note that these tests are not measured for their elemental values, but rather to provide indexes for concrete durability, and have been shown to be sensitive to fundamental material, constructional and environmental factors. A breakdown of the characteristics of each index is shown in Table 2-8 and typical durability index curves for Corex slags are presented in Figure 2-7 on the following page.

Table 2-8 Characteristics of durability indexes

Method	Procedure	Measure	Assessment	Unit
Oxygen permeability test	Falling head permeameter	The rate of pressure decay through concrete sample	State of compaction, presence of bleed voids and channels, and the degree of interconnectedness of the pore structure	- (OPI)
Water sorptivity test	Vacuum saturation facility	The mass of water absorbed from bottom of the sample, due to capillary suction (uni- directional)	Construction quality e.g. the nature and extent of early curing of cover	mm/√h (millimetres per square root of hour)
Chloride conductivity test	Conduction cell	DC conductivity of concrete sample saturated in sodium chloride solution	Resistance of concrete to ingress of chloride ions which induces steel corrosion, e.g. marine and de-icing salt environments	mS/cm (milliSiemens per centimetre)

**Note:** The information in the table above is compiled from the Concrete durability index testing manual (Alexander et al., 1999)

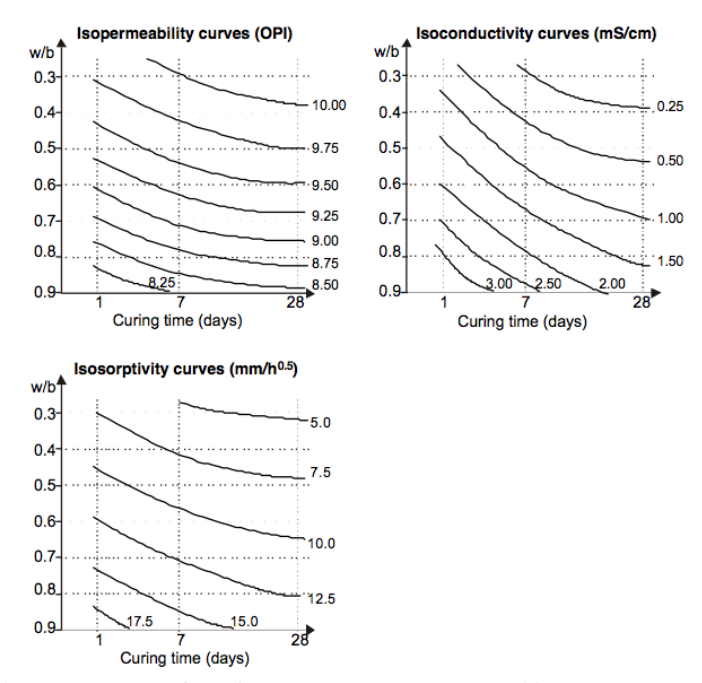


Figure 2-7 Iso-index charts for Corex slag concretes (Alexander et al., 2003, p.23)

Slags historically have been shown to produce good long-term performance, even in under severe environments conditions, and are particularly suited for marine environments due to exceptional chloride resistance above 50% replacement levels.

Apart from the above mentioned durability indexes Alexander et al. (2003) showed that Corex slag concrete displayed a greater resistance to **carbonation** than equivalent PC when accelerated exposure was simulated. Carbonation resistance is favourable as the diffusion of carbon dioxide lowers the pH and induces corrosion. Although there was mention of caution in carbonation measurements of slags due to the lack of long term exposure data. The risk of expansion resulting from **alkali silica reaction** (ASR) was also reviewed, and slags are accepted to reduce the risk of expansion due to the lower pore water alkalinity and the cutback in ion mobility.

#### 2.2.6 Corex technology vs blast furnace technology

In order to fully evaluate the value of Corex slags against blast furnace slags it is important to review the iron production processes that produce these bi-products. The fundamental difference between the Corex process and the conventional blastfurnace process is the combination of the coking plant, sinter plant and blast furnace into a single iron making unit.

The following are the primary benefits of Corex technology:

- Non-coking coal can be used directly as a reducing agent and energy source, eliminating the need for a coking plant
- Up to 80% of the iron oxide fraction can be lump ore, eliminating the need for a sintering plant
- High purity oxygen is used, which results in nearly nitrogen free top gas, and may be recycled for reduction work or used for heat or energy generation.

These primary benefits result in the follow economic and ecological secondary benefits:

- Lower capital investment required due to elimination of the coking and sinter plants
- Lower emission rates
- A wider variety of iron ores can be utilised
- Additional value through generation of highly valuable export gas (dependent on demand)

The introduction of the Corex technology is helping the iron industry meet increasingly stringent environmental regulations and improve economic potential, which will ultimately lead to the goal of long-term sustainable growth.

It is interesting to note that no mention of Corex slags as a cement extender is made in the document released by SIEMENS VAI promoting their technology (Siemens VAI, 2013).

#### 2.2.7 Economic advantages of Corex slag

Apart from the benefits associated with the Corex technology within the iron industry, Corex concretes have been found to have both short and long term economic advantages. The short term advantages are due to the high reactivity of Corex slag which results in a lower total binder requirement for a given grade of concrete. Figure 2-8 show the relationship between the cost of materials for PC and GGCS concretes and the corresponding compressive strength. The long term advantages are based on durability and GGCS slag concretes have been shown to be favourable in harsh marine environments, which translate to lower cost for a required cover depth. Figure 2-9 shows a cost analysis of PC and GGCS concrete, which quantifies the cost advantage of GGCS concretes when cover depth are equivalent. Although PC concrete will ultimately require larger cover depth and therefore further costs may be assumed.

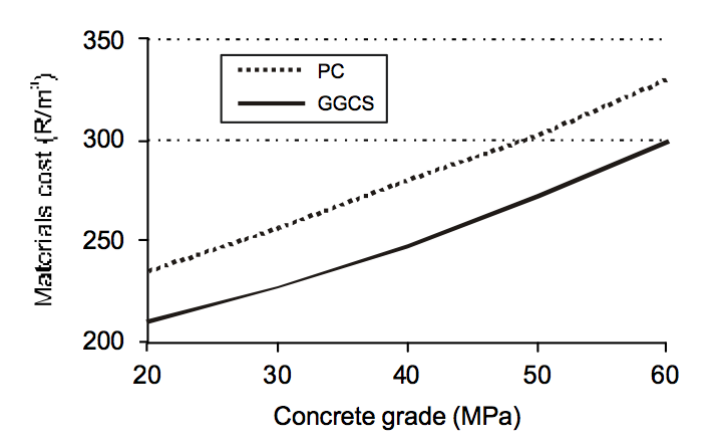


Figure 2-8 Material costs  $(Rands/m^3)$  of concrete for different concrete grades  $(Alexander\ et\ al.,\ 2003,\ p.27)$ 

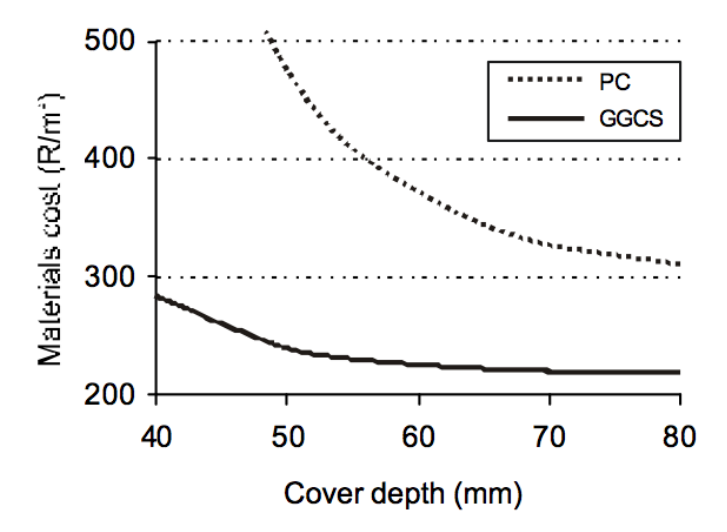


Figure 2-9 Material cost (Rands/m³) for severe marine environment (Alexander et al., 2003, p.27)

**Note:** The materials are based on August 2002 Western Cape prices

#### 2.2.8 Conclusion

Corex slag concrete has been found to exhibit superior structural and durability properties than blastfurnace slag, what may be attributed to its higher reactivity and fineness. Corex slag replacement levels of 50% have been determined optimal based on compressive strength, particularly at early age. The reduction in binder required to produce a characteristic strength of 30 MPa clearly indicates the economic advantage of Corex slag, especially when coupled with the apparent environmental improvements that the Corex technology has on iron production. Setting times will increase with the use slags as latent hydraulic binders react at a slower rate, although Corex slag may have earlier setting times due to higher levels of reactivity than blastfurnace slag. Based on the literature Corex slags do not offer appreciable reductions in the rate of heat development during hydration, which is the case with blastfurnace slag.

#### 2.3 Thermal properties of cement and concrete

The fundamental thermal properties related to cement and concrete, discussed in this section, are as follows:

- Specific heat capacity
- Thermal conductivity
- Coefficient of thermal expansion

These properties give rise to the following aspects:

- Thermal stress development
- Thermal cracking
- Heat liberation (See section 2.4)

#### 2.3.1 Thermal properties

**Specific heat capacity,** with SI units J/kgK, is a measure of the amount of heat energy that is required to elevate the temperature of a unit mass of a specific material by 1°C. Specific heat is sensitive to temperature changes and due to the variant nature of temperature with in concrete structure predictive models are required. In the case of concrete it is commonly accepted practice to use the mass-weighted average specific heat capacity of the concrete constituents. Specific heat values of 880 J/kg.K and 4187 J/kgK for cement and water respectively were used by Ballim and Graham (2009), with regard to their temperature prediction model.

**Thermal conductivity,** with SI units W/mK, is defined as the ability of a material to transmit heat. It is a measure of the quantity of heat transmitted through a unit thickness of material due to a specific temperature gradient. The coefficient of thermal conductivity varies for concrete and is dependent on the moisture content, type of aggregates, density and porosity. Ballim and Graham (2009) mentioned that typical values of thermal conductivity of concrete vary between 1.2 and 3.5 W/mK. It was also stated that although thermal conductivity is temperature dependent the effect is negligible over the range of temperatures associated with concrete construction, but extreme temperature conditions would need to be considered.

Thermal conductivity in concrete varies as the cementing reaction takes place, due the exothermic nature of the reaction as well as the structural change what takes place during the setting process. There is no agreement on the behaviour of this variation and researchers have found conflicting results of both increasing and decreasing values as the reaction takes place. Figure 2-10 below graphically reveals the conflicting results found by different authors.

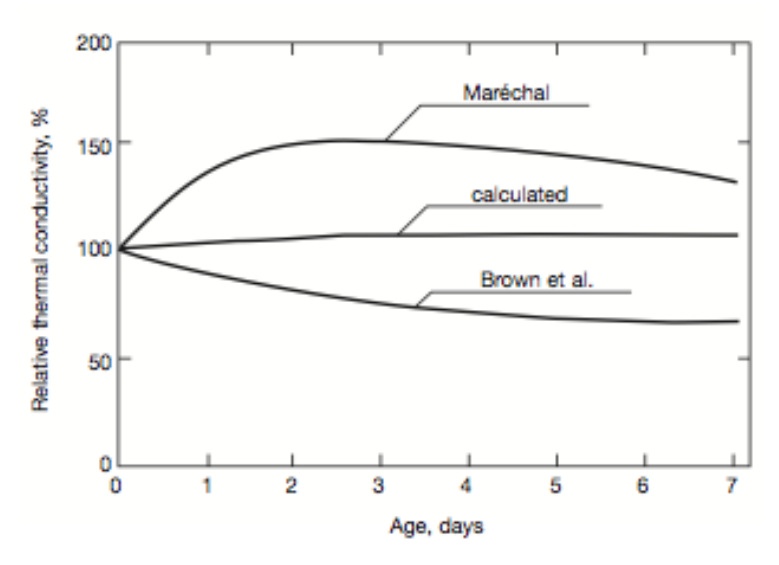


Figure 2-10 Thermal conductivity variations during the early stages of hydration (Ballim & Graham, 2009, p.276)\*

\*Note: The results presented above are from different authors and compiled by van Breugel (1998)

#### 2.3.2 Thermal cracking

The chemical reactions associated with the formation of hardened concrete are exothermic. The heat is liberated by the reacting cement and extenders, which results in highly dynamic thermal gradients throughout the curing process. This reaction is of particular importance due to the heat differential between two points, which may result in thermally induced cracks.

The potential for thermal cracking, as described by Ballim and Graham (2009), is determined as follows:

- Stress induced by strains resulting from transient temperature and shrinkage gradients in the concrete
- Ability of the concrete to respond to these stresses without cracking
- Nature and degree of restraint

Concrete is a composite material that is far stronger in compression than tension, therefore concretes ability to resist cracking due to deformation is directly related its limited tension strength capacity. Tensile strength although being the primary characteristic related to cracking is not the only parameter; relaxation capacity and stiffness also play key roles. The stiffness of concrete increases as the cementing reactions progress and as a result stresses are more easily developed. The increase is stiffness is logically associated with a decrease in the relaxation capacity because the concrete begins to resist deformation. This behaviour necessitates an understanding of the mechanical and thermal properties of concrete throughout the curing process in order to mitigate the potential for cracking that result from the stresses development.

Temperature gradient predictions within concrete elements are of particular importance especially at early ages, where heat liberation is at a maximum. Adequate interpretations of temperature distribution within time and space will enable the analysis of likely stress distributions. This information is useful in determining location specific mechanical properties within a structure for design purposes. This information is also useful to contractors in planning activities, especially with regards to large quantity concrete placement.

#### 2.3.3 Thermal stress development

The thermal movement of concrete is associated with the **coefficient of thermal expansion**, which is the magnitude of strain induced by a unit change of temperature within a material. SANS 10100 (2000) recommends a linear expansion value of 10 x 10<sup>-6</sup>/°C for most structural uses, although it is recommended that thermal expansion is measured directly for stress and deflection sensitive structures (Ballim & Graham, 2009). Thermal expansion is closely related to moisture content and therefore lower levels of thermal expansion are associated with concrete where water absorption is minimal.

Stresses that form in concrete due to thermal expansion and contraction are directly related to the degree of restraint imposed on a structuring while curing. The restraint of a structure can be classified as either **external** or **internal**.

An **external restraint** is formed when fresh concrete is cast directly against a rigid surface and therefore movement is restricted due to the chemical or mechanical connection that forms at the interface. A common example of such a restraint occurs when casting a wall onto a hardened floor slab. The initial elevation in temperature induces a compressive stress at the base of the wall as the concrete expands and is restrained due to the chemical interlock between the mature concrete slab and the setting concrete wall. The compressive stress is low because of the high relaxation capacity of concrete at the early stages of setting. The stress transitions from compression to tension during the cooling phase of the concrete as the wall contracts and is again restrained by the floor slab. Cracking occurs when the stress in the concrete reaches the tensile strength of the concrete in the wall. Figure 2-11 on the following page illustrates the formation of an external restraint due to a wall being cast onto a previously hardened slab.

Internal restraints result due to temperature differentials within the concrete. When there is an uneven distribution of temperature the non-linear rate of expansion and contraction with in a structure causes stresses to develop. This form of restraint is often seen at the surface of concrete, which may cool faster than the internal concrete due to low ambient temperatures. This results in the surface cracking in tension as the internal concrete expands at a faster rate during the heating phase of the reaction. The damage caused due to the surface cracks is mostly cosmetic as the penetration is shallow and the cracks are reduced when the concrete contracts while cooling. Alternatively when the internal concrete core cools it is restrained by the cooler surface concrete and tensile stress may form. If the tensile stress induced reaches the tensile strength of the concrete, internal cracks will form. If the cracks are sufficiently distributed the water-retaining capabilities of a structure can be compromised and the failure potential of load baring elements becomes more prominent (Ballim & Graham, 2009). Figure 2-12 on the following page represents the stress and temperature development over time of a large concrete element.

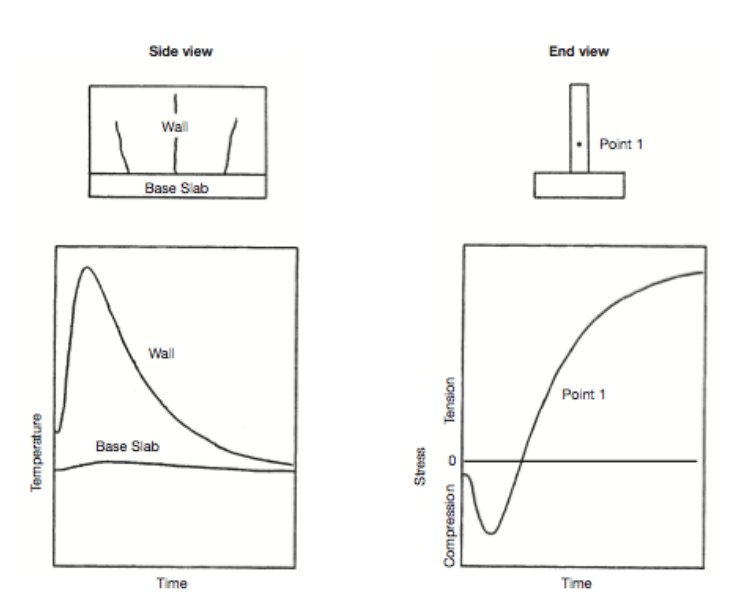


Figure 2-11 Example of the formation of an external retains resulting from casting a wall onto a previously hardened slab (Ballim & Graham, 2009, p.274)

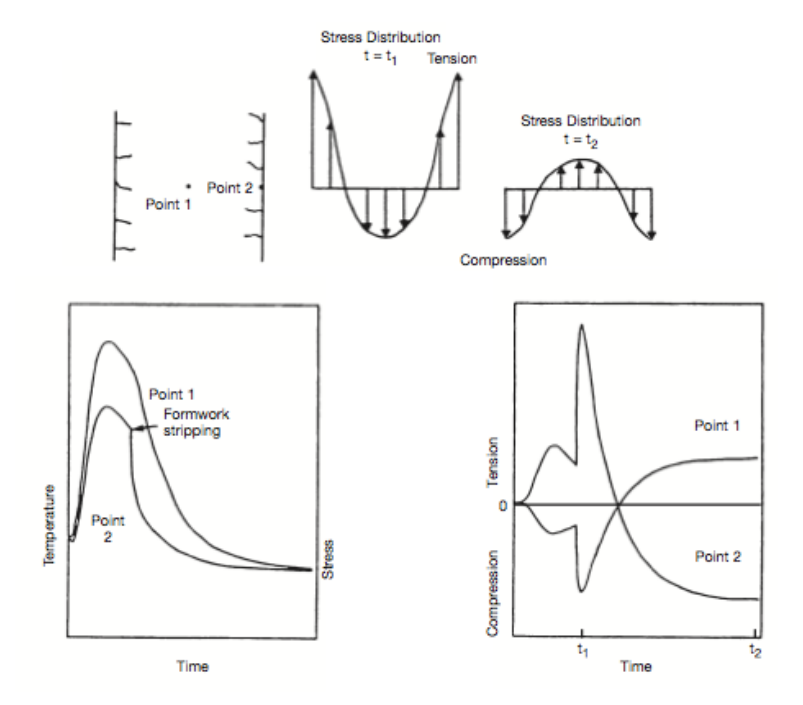


Figure 2-12 Formation of stresses within a large concrete element induced by internal restraints caused by a non-uniform distribution of temperature (Ballim & Graham, 2009, p.275)

#### 2.3.4 Conclusion

The exothermic nature of the hydration reaction of cement results in highly dynamic thermal gradients within curing concrete. This characteristic of concrete is important because heat differentials may thermally induce cracks. A coefficient of thermal expansion of 10 x 10<sup>-6</sup>/°C is recommended for concrete, although moisture prone and deflection sensitive structures may require direct measurements. The specific heat capacity of concrete is calculated using the weighted average of the constituents, but is sensitive to temperature changes and therefore temperature prediction models are required for curing concrete. The thermal conductivity of concrete typically varies between 1.2 and 3.5 W/m.K with temperature changes having a negligible effects within the temperature range of concrete structures. The stresses that ultimately develop due to thermal expansion are as a result of external and internal restrains on a structure.

#### 2.4 Determination of heat liberation in cementitious binders

As mentioned in section 2.1.5, the rate of heat evolved varies within a series of phases over time (see Figure 2-2) at normal hydration temperatures. In the case of temperature modelling of large concrete elements at early ages, the heat evolved as a result of phase 1 is ignored due to the following assumptions (Ballim & Graham, 2003):

- The reactions take place before the concrete has been placed into the formwork
- The heat liberated is small and has little effect on changing the temperature of concrete at time of placing.

The rate of heat evolved during Phases 2 and 3 have been modelled by guide equations and other more complex models based on the chemistry and crystallography of cement, but laboratory test measurements have been found to be more reliable (Ballim & Graham, 2009). The heat evolution of reacting cement and extenders has been measure using a variety of methods. The methods are defined by three different groups of calorimetry: isothermal, semi-adiabatic and adiabatic.

A definition of each method of calorimetry is as follows:

- **Isothermal** methods attempt to measure the heat generated during a reaction where the sample is kept at a constant temperature
- **Semi-adiabatic** methods monitor the heat liberation of a reaction while attempting to limit the heat exchange between the sample and the environment but not entirely preventing it
- Adiabatic methods aim to eliminate the heat exchange between the sample and the environment as far as possible during the reaction.

Isothermal and semi-adiabatic calorimetry pose a problem as the rate of heat liberation is influenced by temperature; therefore the heat lost to the environment is not able to contribute to the temperature of the sample and ultimately the rate of heat evolution is affected. For this reason adiabatic calorimetry is favoured by researchers attempting to limit this heat exchange between the environment and test sample.

Apart from largely eliminating the heat exchange between a test sample and the environment, adiabatic calorimetry is also convenient, easily reproducible and a practical procedure, given that the equipment is of sufficient quality. Adiabatic conditions are said to exist at depths of 0.5m within mass concrete (Ballim & Gibbon, 1996) and therefore measurements taken using adiabatic calorimeters are favoured when considering prediction models of mass concrete.

#### 2.4.1 Isothermal calorimetry

The ASTM Standard practice for measuring Kinetics of hydraulic cementitious mixtures using isothermal calorimetry describes a method for measuring the relative differences in hydration kinetics of hydrating cementitious mixtures (ASTM, 2009), either of paste or mortars. Variations in mixes may include different admixtures, supplementary cementitious materials (SCM), other fine materials or a combination of these materials. Comparisons are done by measuring the thermal power using an isothermal calorimeter.

The isothermal calorimeter consists of a heat sink with a thermostat, two heat flow sensor and a sample vial holder which is attached to each senor. One vial contains a fresh sample mixture and the second vial holds a thermally inert mixture of sand and water with similar thermal properties as the active sample. The heat produce by the hydration of the active sample is transferred and passes across the heat flow sensor. The output from the calorimeter is calculated from the difference between the outputs of the heat flow sensors from the active and inert samples. The heat is allowed to flow away for the sample therefore the measurement will be taken at an approximately constant temperature. This characteristic defines the calorimeter as isothermal.

The thermal power curves that are developed can be used to evaluate the isothermal hydration kinetics of the combined mixtures of various materials during the early stages after water addition. These hydration profiles can be used to evaluate the following:

- Relative setting characteristics (based on final time of set)
- Material compatibility
- Sulphate balance
- Early strength development
- Effects related to composition, proportions and time of addition of materials
- Curing temperature

#### 2.4.2 Semi-adiabatic calorimetry

It is nearly impossible to conduct "perfect" isothermal or adiabatic calorimetry tests without specialised equipment, which may be costly in most cases. A hybrid termed semi-adiabatic calorimetry is thus employed frequently to describe a simple more cost effective means by which to measure the heat of hydration. Cost (2008) described semi-adiabatic calorimetry, in a presentation at the TTCC/NCC Conference, as an indication of the heat evolved from a cementitious mixture hydrating in an environment or container having some thermal insulation properties, according to a record of the mixture's changing temperatures over time. He went on further to define the properties of a semi-adiabatic calorimeter as follows:

- The value is generally in comparative data
- Simpler, less expensive equipment is required
- Results are affected by certain variables
- Useful in the field or the laboratory

Simple semi-adiabatic calorimeters can be constructed on relatively low budgets for use in the field or in the lab for many practical applications. Cost (2008) makes mention of the following applications:

- Comparing setting time effects and hydration efficiency
- Troubleshooting concrete field problems
- Cement quality control (optimizing sulphate content)

Apart from the above mentioned applications work is being done by ASTM to develop an alternative time of set method (See section 2.4.4) by using semi-adiabatic calorimety to replace test method C403 (ASTM, 2008)

The figure below shows a typical low budget semi-adiabatic calorimeter setup which is relatively easy to reproduce.



Figure 2-13 Typical Semi-Adiabatic calorimeter (Cost, 2008)

#### 2.4.3 Adiabatic calorimetry

It is near impossible to achieve a 'fully' adiabatic environment; therefore a calorimeter is only considered to be adiabatic when temperature losses of samples are not higher than 0.02 K/h (CP Tech Center, 2006). In order to prevent heat loss the surrounding environment needs to be controlled through providing insulation, heated containers or a combination of both. Adiabatic heat measurements are particularly useful in producing continuous heat of hydration curves which can be related to mass curing conditions, and it is this characteristic of adiabatic calorimetry that makes it the most practical for temperature predictions in hardening concrete. Ballim and Graham (2009) made use of a low cost adiabatic calorimetric system to obtain the rate of heat evolution of concrete, which was then transferred as input into a model to calculate the heat gradients within early age concrete. This temperature prediction model is discussed in section 2.5.

In general the shape of the temperature profiles generated by semi-adiabactic calorimeters are initially similar to those of a fully-adiabatic system. However the profiles diverge as the heat losses increase and a peak is formed in the semi-adiabatic profile, which usually occurs within 24 h. The fully adiabatic profile continues to increase but the rate of the temperature rise decrease significantly after 24 h. A graphical representation is of this behaviour can be seen in Figure 2-14 on the following page.

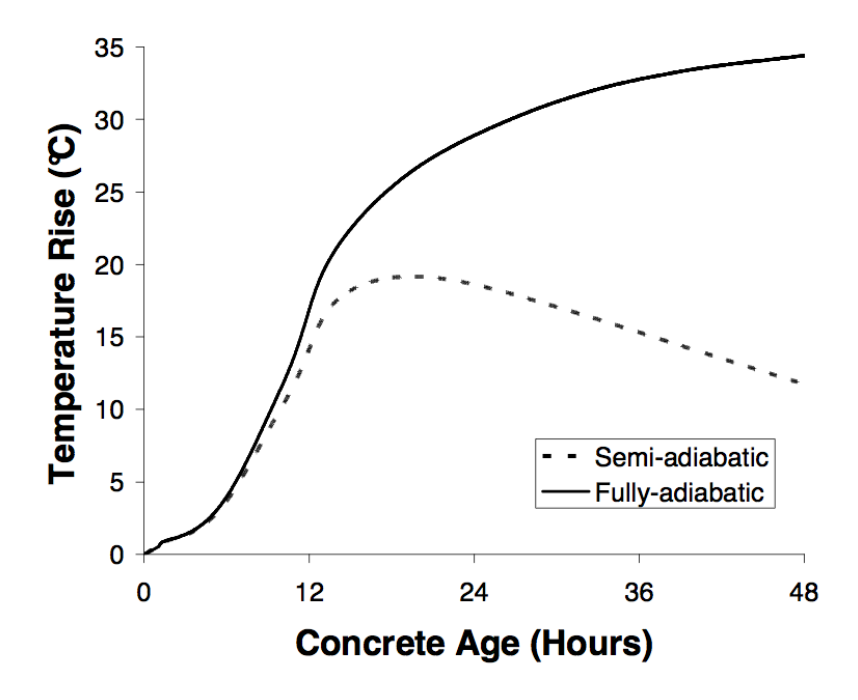


Figure 2-14 Example of semi-adiabatic and fully-adiabatic temperature profiles (Weakley, 2010)

#### 2.4.4 ASTM thermal measuring <u>draft</u> standard

ASTM international has developed a draft standard for the evaluation of hydration of hydraulic cementitious mixtures using thermal instrumentation. This draft is in the early stages of development under a task group within Subcommittee C01/C09.48 and has not yet become a ASTM standard, but in the context of this report it is being used as guide line. Information is provided on how to use simple thermal measurements to evaluate the early age hydration of concrete, mortar, or cement pastes. The materials may be combinations of cement, pozzolans, slags and chemical add mixtures, which may or may not contain aggregates.

This standard will be useful in determining

- time of set
- early hydration rates
- abnormal hydration tendencies

The intent of this practice is to serve as a tool for comparison of different test sample and their relative performance when tested under similar conditions. Although this practice is similar to isothermal or semi-adiabatic calorimetry it is not intended for cross examination of different laboratory equipment as no quantifiable measurements are provided for actual hydration rates.

#### **Background to practice**

An inert specimen is placed in the same thermal environment as the test sample and is made up of nonreactive material of similar thermal properties and mass as the sample specimen. The temperature difference between the nonreactive and hydrating specimen will be representative of the heat due to hydration. The thermal profile is developed by subtracting the test specimen's temperature from the inert control specimen, which can be seen in the figure below.

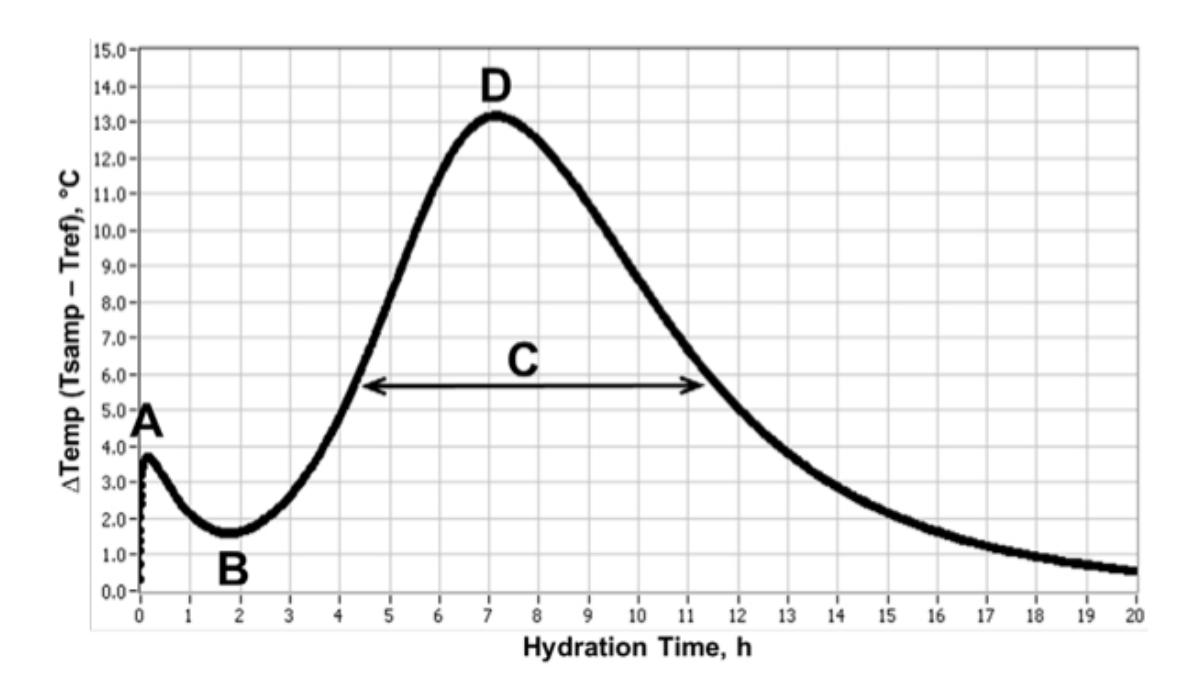


Figure 2-15 Thermal profile of a Portland cement paste where the inter sample temperature has been subtracted (ASTM draft, 2012)

The shape of the curve is described as being influenced be the following parameters:

- mixture hydration
- Sample type
- Sample container size and shape
- Provided insulation around sample container
- The relative surrounding environment temperature.

#### **Summary of procedure**

The basic requirements for the experimental procedure are temperature measuring devices (thermocouples), data collection equipment and software to interpret the data, and sample containers capable of insulating test specimens, for both the hydrating and inert samples.

Thermal data collection should be initiated as fast as possible after the test specimen has been prepared, which may comprise of cementitious materials, water and optional admixture and aggregates. From the thermal data collected thermal profiles can be plot to allow for comparison of the hydration properties of each sample. The test and inert sample must be maintained within a reasonably constant ambient temperature, which is to be recorded throughout the experimental period. Graphical comparisons of the recorded data must be done within a common time scale and should be initiated after mixing water is introduced to cementitious materials.

The procedure offers indications of the following properties:

- Relative setting characteristics
- Compatibility of different materials
- Sulphate balance
- Heat of hydration
- Early strength development

These properties can be used to evaluate the effects such as composition, proportion and ambient temperature, which are useful to concrete producers, material suppliers, contractors, mix design development and evaluating filed related issues. Although thermal testing can help in understanding concrete issues such as setting time and slump loss, it does cannot provide a complete performance prediction. Thermal testing is better suited to the evaluation of setting trends with regard to mortars and concrete, but the ASTM draft standard (2012) did mention that paste sample of similar proportions can be equally useful.

The apparatus as required by the ASTM draft standard (2012) for preparing samples are as follows:

- Weights and weighing devices that satisfy the requirements of ASTM specification C1005, and are required to be accurate to 0.1g with a minimum load capacity of 1000g
- Graduation cylinders that satisfy specification C1005
- Mixing equipment should produce a uniform mixture

With regard to the thermal measuring equipment the draft standard does allow for variations in the actual design of the equipment, which may be commercial or custom-built. However a signal-to-noise ratio of no less than 5 is required. Where the signal is define as the temperature difference between the minimum and maximum values of the hydrating sample, whereas the noise is the difference between the highest and lowest temperature value for the inert specimen. The signal and noise values are represented graphically in the Figure 2-16 on the following page.

The type, size, mass of sample, insulation of container, initial mixture and test temperature will influence the peak response values and the proposed standard emphasise the importance of balancing these factors in order to meet the signal noise ratio

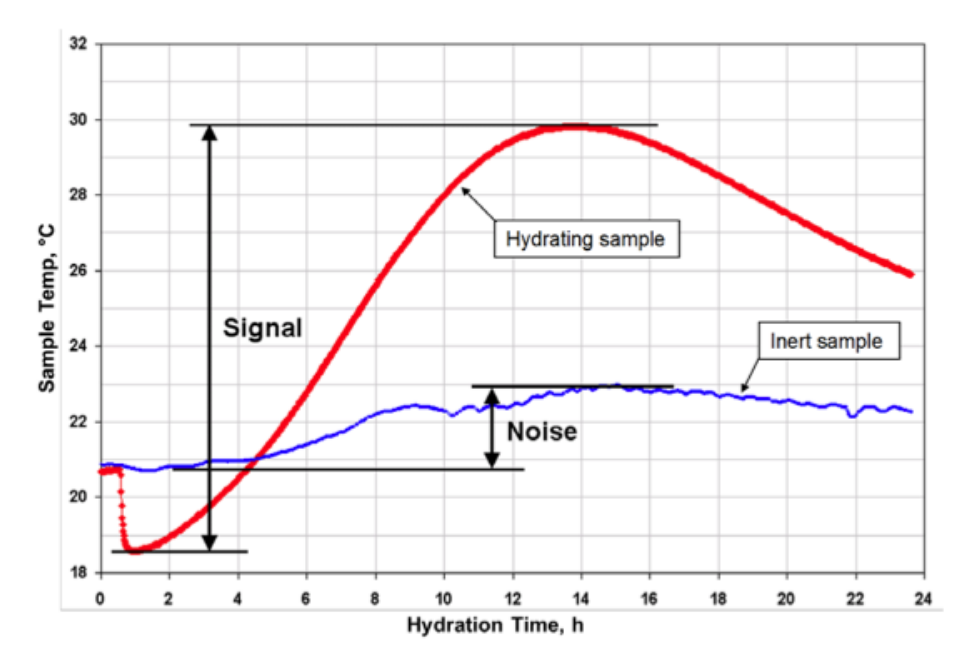


Figure 2-16 Signal and noise determination for verification of minimum ratio (ASTM draft, 2012)

The draft standard also outlines a method to approximate the **setting time** of concrete base on a fraction of the main peak response of the thermal profile. The main peak response is defined by the primary temperature increase in the thermal profile that begins at the end of the dormant period, and if a sulphate balance is present this may last for several hours. Relative setting times may be compared by evaluating the timing of the main peak response among mixtures within the same test series. There may be variations in the magnitude and shape of the thermal profiles as a result of chemistry or fineness differences of various materials or proportions. For this reason the most consistent tool for comparison is the use of a chosen percentage of the main peak response which correlates to the setting time mark. The fraction chosen can be determined from actual setting time results, where essentially the thermal profile is calibrated to determine setting times. The lowest temperature of the dormant period may be difficult to determine or may even be missing (common in actual project concrete), in such cases estimates can be made based on the available data, assuming that at typical thermal profile forms. Figure 2-17 on the following page illustrates the use of a 20% and 50% fraction of the main peak response to determine the approximate initial and final setting times respectively.

It appears that ASTM is developing a standard that is relatively simple and cost effective to conduct. This standard, when published, should offer the means by which to compare the hydration behaviour and possibly even setting times, of different mortar, concrete and cementitious pastes. Although the actual heat of hydration is not determined by this practice, it is still useful in developing relative classification of materials and in helping troubleshoot issue on site.

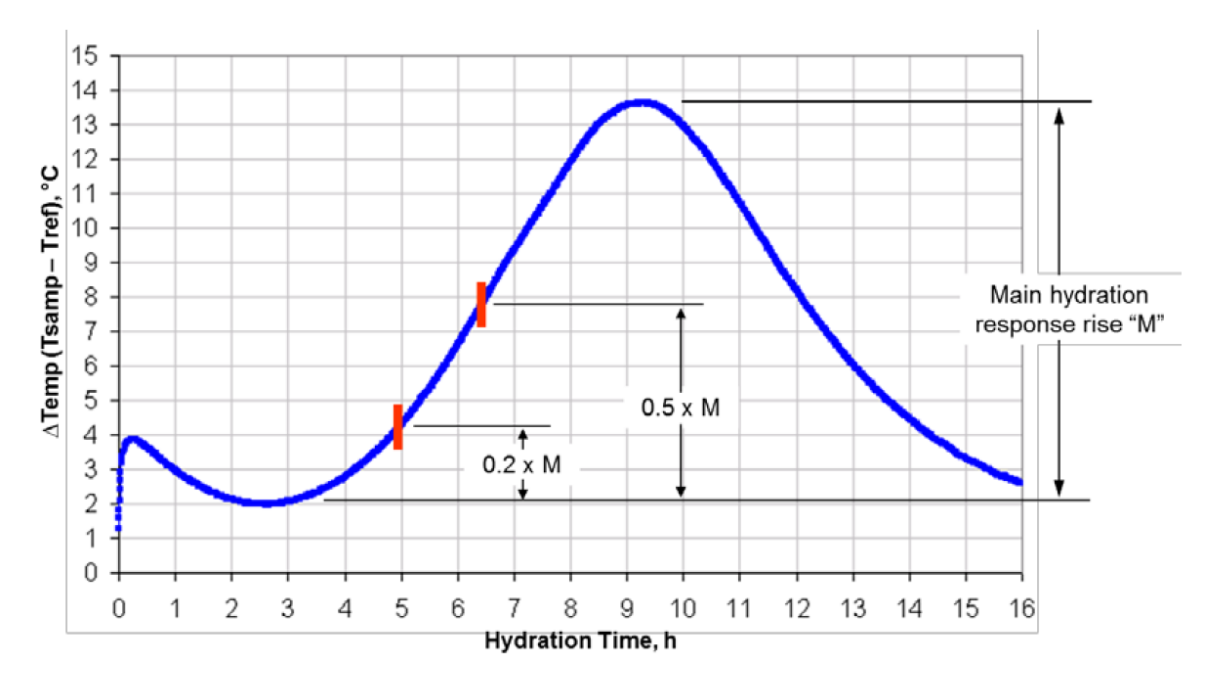


Figure 2-17 Setting time mark shown at 20% and 50% fractions of the main peak response temperature rise of a typical concrete mixture (ASTM draft, 2012)

#### 2.4.5 Conclusion

Adiabatic calorimetry is the most useful method for measuring the heat of hydration as heat exchange is limited. Isothermal and semi-adiabatic calorimeters don't account for heat lost to the environment which is problematic because the rate of heat liberated is influenced by temperature. For this reason adiabatic calorimeters better simulate the heat profile of concrete curing within a structure. Although semi-adiabatic calorimeters appears to be the most incomplex and cost effective method to develop thermal profiles. However the data collected through is method is limited in that comparisons can only be made between samples measured with the same calorimeter under the similar environmental conditions.

# 2.5 Predicting temperature in early age concrete

#### Finite difference temperature prediction model

Ballim and Graham (2009) have developed a numerical model for predicting time-temperature profiles within concrete structures. The flow of heat is predicted using the Fourier equation in a transient two dimensional form, which can be seen below.

$$\rho \times C_p \times \frac{\partial T}{\partial t} = k \times \left(\frac{\partial^2 T}{\partial x^2} + \frac{\partial^2 T}{\partial y^2}\right) + \frac{\partial q}{\partial t}$$
 (2-4)

where:

 $\rho$  = density of the concrete

 $C_p$  = specific heat capacity of the concrete

T = temperature

t = time

```
k = thermal conductivity concrete

x and y = coordinate at a particular point in a structure

q = heat evolved by hydrating cement (J/m^3)

= time rate of heat liberated at a particular point (W/m^3)
```

Temperature at any point in the structure varies with time and position. For this reason the transient form of the Fourier equation is used. The heat evolution rate is also required as input, which becomes problematic as this rate is time-dependent due to the change in the rate of hydration over time. This problem is overcome by expressing the heat rate in terms of the extent of hydration.

The heat of hydration in this model is determined by **adiabatic calorimetry** and described by Ballim and Graham (2005) in a research monograph as follows:

- Immediately after casting, a 1 litre sample of concrete is placed into a water bath, such that the concrete is separated from the water by a stationary air pocket
- A temperature probe is placed into the sample and monitored via an analogue to digital conversion card, which is connected to a personal computer
- The computer switches a heater on and off in the water bath in order to maintain equal temperature between the sample and the water, ensuring no heat is exchanged with the environment around the sample
- The air barrier acts as a harmonic dampener for any heat exchange between the sample and the water due to the sensitivity of the thermal probes
- At 7 days the heat evolution is said to be too low for the thermal probes to pick up and therefore the test is usually terminated at this time

Below is a schematic diagram of the calorimeter as presented in the monograph (Ballim & Graham, 2005).

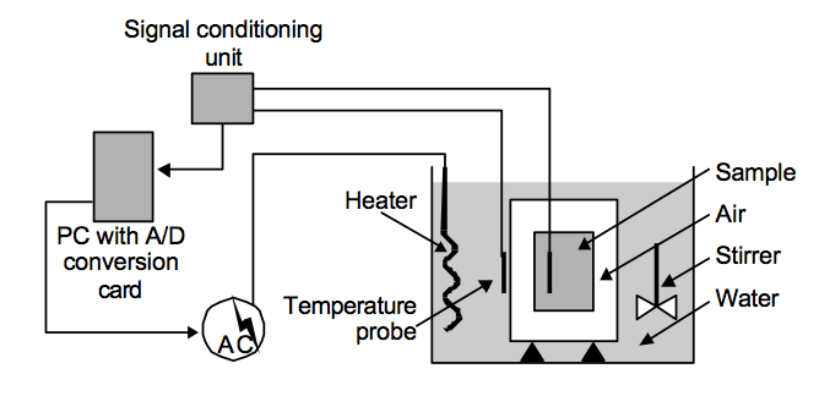


Figure 2-18 Schematic of adiabatic calorimeter arrangement (Ballim & Graham, 2005, p.12)

This test measures the change in temperature of the concrete sample over time. Therefore the total heat per unit mass of binder that is generated at a specific time, during the experiment, can be approximated from the equation below.

$$q_t = C_p \times (T_t - T_o) \times \frac{m_s}{m_c}$$
 (2-5)

where:

 $C_p$  = specific heat capacity

 $T_t$  = temperature of the sample at time t

 $T_o$  = temperature of sample at the beginning of the test

 $\frac{m_s}{m_c}$  = ratio of concrete mass in test sample to binder mass in sample

The rate of heat liberated during the hydration process can be calculated by differentiating equation 2-5 with respect to time.

$$\frac{\partial q}{\partial t} = \frac{\delta q}{\delta t} = \dot{q}_t \tag{2-6}$$

(Units of J/s.kg or W/kg)

A "typical" total heat and heat rate curve of a South African Portland cement, measured by an adiabatic calorimeter (WITS University), is presented in the figure below.

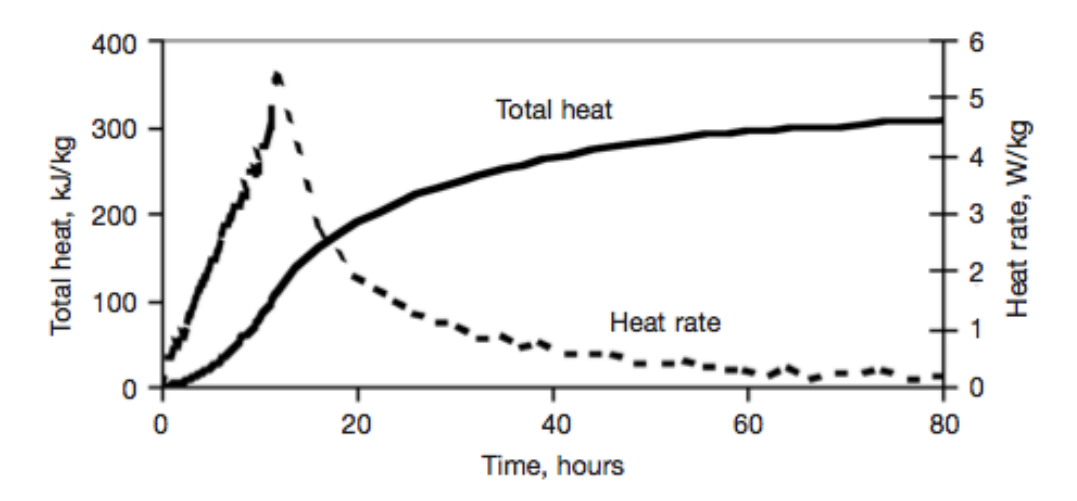


Figure 2-19 Local Portland cement heat curves (Ballim & Graham, 2009, p.278)

## Maturity approach to the rate of heat liberated

The rate of heat evolved  $\dot{q}_t$ , which is represented by equation 2-6 above, is required as input into the Fourier equation (see equation 2-4) in order to determine the temperature distribution across a modelled element. However, the heat rate curves produced from calorimeter measurements only apply to the unique temperature conditions of the cement sample. Different points in a structure are expected to experience varying time-temperature histories and therefore different  $\dot{q}_t$  values. In order to solve this problem the heat rate, rather than in a

clock-time form, is expressed in the extent of maturity. Ballim and Graham (2003) proposed the use of the Arrhenius form of maturity based on Naik (1985), which is presented below.

$$M = \sum_{i=1}^{i=n} exp\left[\left(\frac{E}{R}\right)\left(\frac{1}{293} - \frac{1}{273 + 0.5 \times (T_i - T_{i-1})}\right)\right] \times (t_i - t_{i-1}) = t_{20}$$
 (2-7)

where:

M = equivalent maturity time based on concrete cured at 20°C

E = activation energy parameter, which is taken as a constant of 33.5 kJ/mole

(Bamford & Tipper, 1969)

R = universal gas constant of 8.314 J/mole

 $T_i$  = temperature in  ${}^{\circ}C$  at the end of the  $i^{th}$  time interval

 $t_i$  = clock time at the end of the  $i^{th}$  interval

By expressing the heat rate curve as a maturity rate of the heat liberated  $(\frac{\partial q}{\partial M})$ , it is normalised and the heat rate curve in this form can now be used as input into Equation 2-4 in order to determine solutions for the time-temperature model. The time-based heat rate at a particular point in a structure can be derived from the following expression:

$$\frac{\partial q}{\partial t} = \frac{\partial q}{\partial M} \times \frac{dM}{dt} \tag{2-8}$$

It can be seen from Equation 2-8 above, that both the maturity development and the rate of change of maturity need to be monitored at each analysis point in a structure. The figure below shows the same curve as represented in Figure 2-19 expressed in maturity form, suitable for use in numerical solutions to Equation 2-4.

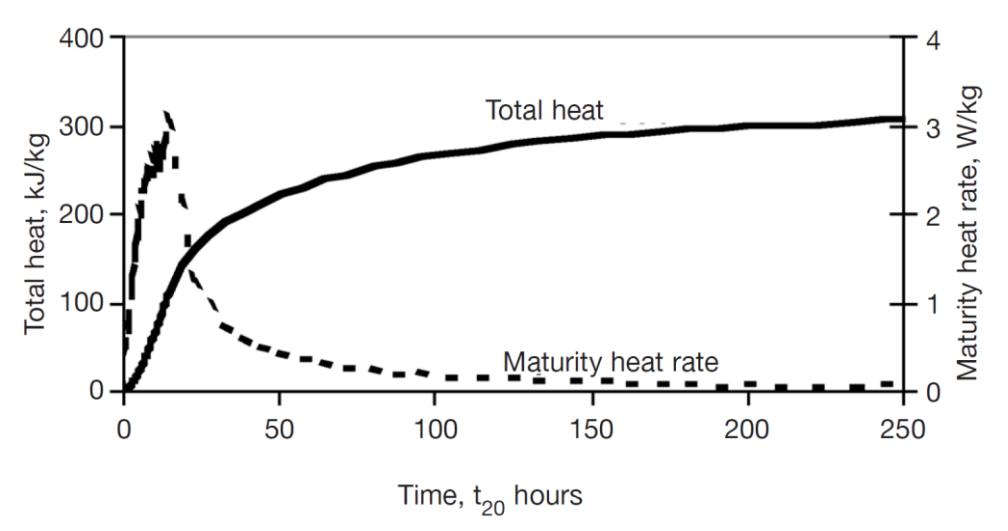


Figure 2-20 The heat curves of Figure 2-14 expressed in maturity form (Ballim & Graham, 2009, p.279; Grieve, 2009; Grieve, 2009)

#### 2.5.1 Conclusion

The model developed by Ballim and Graham, for predicting time-temperature profiles within concrete structures, require the direct experimental measurement of the thermal profile generated by the constituents of the concrete in question. Although pre-determined thermal measurements of standard constituents may be used to estimate thermal behaviours. However the use of any irregular constituents may require direct adiabatic measurements in order to provide sufficient accuracy.

## 2.6 Methods of assessing setting time

Two standard methods of accessing setting time are review, with the first being SANS 50196-3 (1994) and the second ASTM C403/403M - 08 (2008). The fundamental difference between the two methods is that the first relates directly to cement while the second relates to concrete directly.

#### 2.6.1 SANS 50196-3:2006

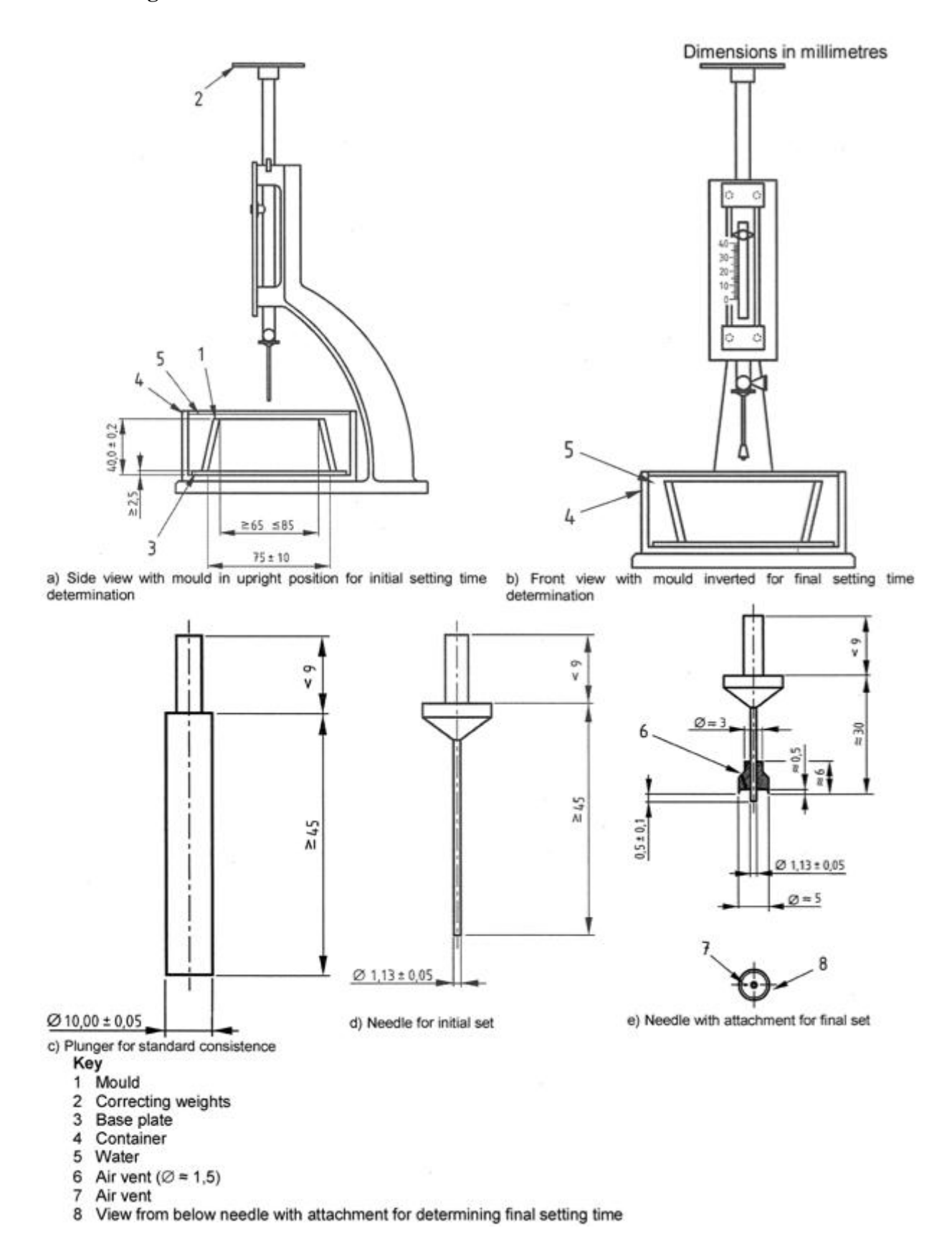
The standard specifies a method by which to determine the standard consistence, setting times and soundness of cements. It can be applied to all common cements and other cements and materials, with the exception of cement with very short initial setting time. Ultimately this method assesses whether the setting time and soundness of cement conforms to its specification.

Only the standard consistence and setting times are reviewed as soundness is not in the scope of this of this research document. The standard consistence of a cement paste has a specific resistance to a standard plunger. The w/b ratio for standard consistence is determined by means trial penetration with varying water contents. In order to determine the setting time a cement paste sample of standard consistence needs to be prepared. Setting time is defined by observing the depth of penetration of a needle into the cement paste sample until it reaches a define value. Both the standard consistence and time of setting tests are perform with a manual Vicat apparatus as shown in Figure 2-21 on the following page.

#### 2.6.2 ASTM C403/C403M - 08

This standard specifies a test method for determining the time of setting of concrete, with a slump above zero, as well as mortars and grouts. This is done by means of the penetration resistance of mortars sieved from concrete mixture or mortars and grouts directly. This method consists of placing a mortar sample in a container and storing it at a specified ambient temperature, after which penetration by standard needles are measure at regular interval. The initial and final setting time are then determined by assessing the plot of penetration resistance against elapsed time. This method may be used to determine the effects of variations on the setting time of concrete such as water content, type and amount of cementitious material or admixture.

Figure 2-21 Typical manual Vicat apparatus for determination of standard consistence and setting time



## 2.7 Main findings of literature

The literature revealed the highly dynamic nature of temperature development in early-age concrete, making it an extremely difficult material to model. The heat of hydration is dependent on the composition of cement and the proportion of extenders forming the cementitious material. The most important parameter in modelling time-temperature gradients within concrete elements was found to be the rate of heat liberation due the exothermic nature of the hydration reaction. The literature has found that the guide equations that have been developed to determine the heat evolved during hydration are not reliable enough, and experimentation is required in order to provide the accuracy needed for time-temperature prediction models.

There are multiple experimental methods to determine the heat liberated during the curing process, but the ambient temperature of the environment in which the experiment takes place effects the rate of hydration and therefore the rate at which heat is liberated. As a result careful control of the environment is required in order to produce quantifiable heat rate measurements. This requires a specialised setup which may be costly but simpler methods can provide a means by which to compare different samples which are tested under the same conditions. Ultimately an adiabatic calorimeter is the preferred method of measuring quantifiable heats of hydration

Semi-adiabatic and isothermal methods of calorimetry produce thermal profiles that are used on a relative basis to determine variations in concrete/cement for means of classification and quality control. The direct use of thermal measurements by calorimetry in the concrete industry is growing but there is still a lack of standardisation with regard to the calorimetric setup. Standard practices are being produced but they allow for large variations in thermal measurements, this is due to the complexities in the heat of hydration process of cemetitious materials and the difficulties associated with controlling the experimental environment. Until the use of thermal analysis of cemetitious materials becomes prominent within the concrete industry high quality calorimeters are likely to be very costly or require high skill sets for custom build systems.

Corex slags have been found to show a higher reactivity rate and therefore increased thermal hydration profiles than those of ordinary blastfurnace slags, which may result in unexpected variations to mix designs if industry is not made aware of these characteristics. Apart from the benefits associated with the Corex technology within the iron industry, Corex concretes have been found to have both short and long term economic advantages. Based on the environmental, economic and structural advantages of Corex slags it is easy to assume that this material as an extender in the concrete industry is likely to expand.

# 3 Experimental methodology

Overviews of the experimental processes are outlined in this section, which consists of the following:

- Proportioning of the sample mixtures
- Mixing procedure
- Standard consistence and setting time tests
- Semi-adiabatic calorimetric procedure

Further detail of the experimental procedures can be seen in the Appendices.

## 3.1 Cement paste proportion

In order to produce well defined peak responses in the temperature profiles, cement paste mixtures of low w/b ratio were chosen, which also closely relates to the water content required to produce a standard consistence (SANS 50196-3, 2006). This allows for a direct comparison between the thermal profile and the measured setting times. Mixture 1 consists of 100% PC (CEM I 52.5N) and a 50% slag substitution for mixtures 2 and 3 were selected based on the favourable properties found with concrete of this proportioning (Alexander et al., 2003).

 Mix proportions % – w/b = corresponding to consistence test

 Mixture
 M1 - PC
 M2 - BS
 M3 - CS

 CEM I 52.5 N
 100
 50
 50

 Binder
 GGBS
 50

 GGCS
 50

**Table 3-1 Proportions of experiment mixtures** 

## 3.2 Standard consistence and time of setting

The SANS 50196-3:2006 method of testing cement (see section 2.6.1) was used to determine the standard consistence and setting time of the three cement paste mixtures. This method is used to assess whether the setting time of particular cement is in conformity with its specification. The method for mixing the pastes is clearly defined in standard method (SANS 50196-3, 2006) and the standard consistence is determined through trial and error to give the w/b ratio to be used in the initial and final setting time tests. The initial and final setting tests are conducted through penetration of a sample at standard consistence with the use of a manual Vicat.

## 3.2.1 Summary of experimental procedure

An automatic mixer was used to prepare samples using 500 grams of binder and varied amounts of water to determine the standard consistence. The total mixing time was 3 min 30s, which includes 30s where the automatic mixer was stopped for manual redistribution of the mixture at the midway point. Once the w/b ratio had been determined at standard

consistence, by plunger depth penetration, samples for setting time tests could be prepared. The initial setting time test was conducted by needle penetration at appropriately spaced time intervals ( $\pm 10$  min), which commenced at  $\pm 2$  h after wetting of binder and was terminated once a depth of 6 mm ( $\pm 3$  mm) was achieved between the needle and the base plate of the Vicat. Final setting time was determined by measuring the depth of penetration on the inverse surface of the sample used for the initial setting time test. Again the test was conducted at appropriately spaced time intervals ( $\pm 30$  min), which commenced at  $\pm 3$  h after wetting of binder and was terminated once the final setting time needle penetrated the sample by only 0.5 mm, which is indicated when no marking by the final setting time needle attachment was seen on the surface of the sample.

For a detailed overview of the **apparatus** used and **procedure** followed please refer to **Appendix A**, where the following will be cover:

- Instrumentation
- Mixing procedure
- Steps to determine standard consistence
- Steps to determine initial and final times of set

## 3.3 Calorimetry method

The method of calorimetry chosen for experimentation is semi-adiabatic as the sample environment is insulated with polystyrene, which has a density of 20 kg/m³ and a thermal conductivity of 0.042 (Basyigit et al., 2004). Each sample is contained in a polystyrene flask which is then placed into a polystyrene enclosure for further insulation (see Figure 3-1 below). A 'fully' adiabatic calorimeter would have been preferred as eliminating heat exchange between the sample and the environment is vitally important in accurately approximating the actual heat of hydration produced by the mixture. Ballim and Gibbon (1996) successfully construction of a low cost adiabatic calorimeter but due to time constrains and the complexity of the system a simpler method was pursued. Furthermore due to budget constrains an 'off the self' calorimeter was not plausible.



Figure 3-1 Semi-adiabatic calorimeter insulation

The setup of the semi-adiabatic calorimeter is based on the guidelines defined in the ASTM draft standard (2012) and advice obtained from Dale Bentz of the National Institute of Standards and Technology (NIST, USA).

The experiment took place under laboratory conditions where the temperature  $(20^{\circ}\text{C} \pm 2)$  and relative humidity (not less than 50%) was controlled. All materials and instrumentation used were acclimatized to the experimental environment before batching and data logging commenced. Mixtures were monitored separately and two temperature profiles were developed from two 650g samples (e.g. M1A- PC and M1B - PC). For each of the three mixtures the temperatures of an inert sample and two hydrating samples were monitored over 24 h, during which time the environmental conditions were kept constant. The sample mixing procedure was identical to that followed for the standard consistence and setting time tests, which is outline in SANS 50196-3 (2006). An image of the semi-adiabatic calorimeter and the DAQ system configuration diagram can be seen in

Figure 3-2 and Figure 3-3 respectively.

# 3.4 Cost breakdown of semi-adiabatic calorimetric system

The table below shows a cost breakdown for a semi-adiabatic calorimeter based on 2013 prices. The DAQ system quoted is from Measurement Computing and has 8-channels for thermocouple input and data is collected directly via USB. This system is more convenient then the DAQ system used during experimentation due to the following:

- Less equipment is required
- The system is easily mobile and a laptop with a USB connection is sufficient
- An independent DAQ board is not required allowing any computer to be used for data acquisition
- No specialised connection cables are required
- Software is freely downloadable

Higher quality insulation (lower thermal conductivity) may be used to further reduce heat losses, although a temperature regulation system is usually required to achieve a fully adiabatic system.

Table 3-2 Estimated cost breakdown of semi-adiabatic calorimetric system

Cost breakdown				
Equipment	Cost per unit (R/unit)	Quantity	Cost (R)	
Polystyrene block	100	1	100	
Polystyrene flasks	10	8	80	
Thermocouples	380	6	2280	
DAQ system	3900	1	3900	
	6360			
Labour	$\approx 100  (R/h)$	$\approx 1$ (h/sample set)	100	

For a detail overview of the **apparatus** used and the **procudure** followed please refer to **Appendix B** 

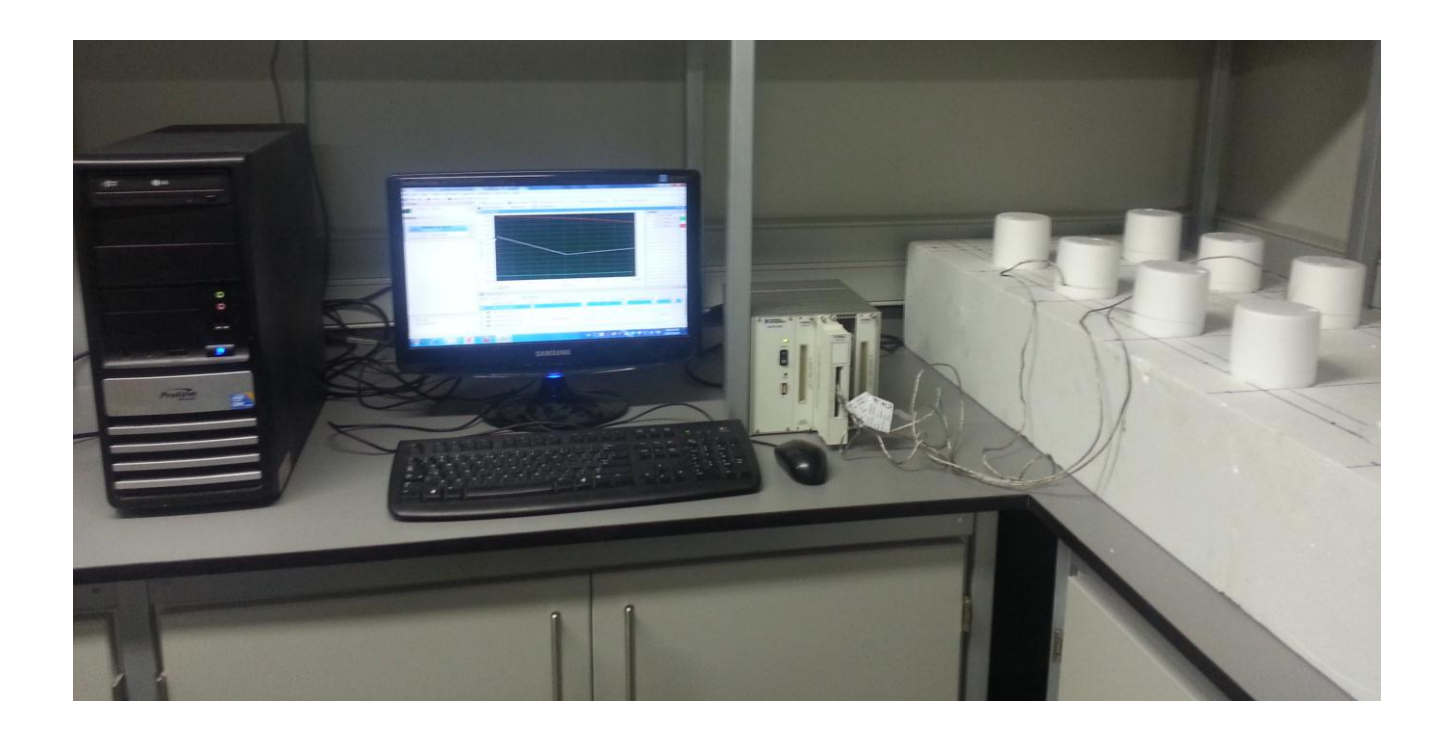


Figure 3-2 Experimental setup of semi-adiabatic calorimeter

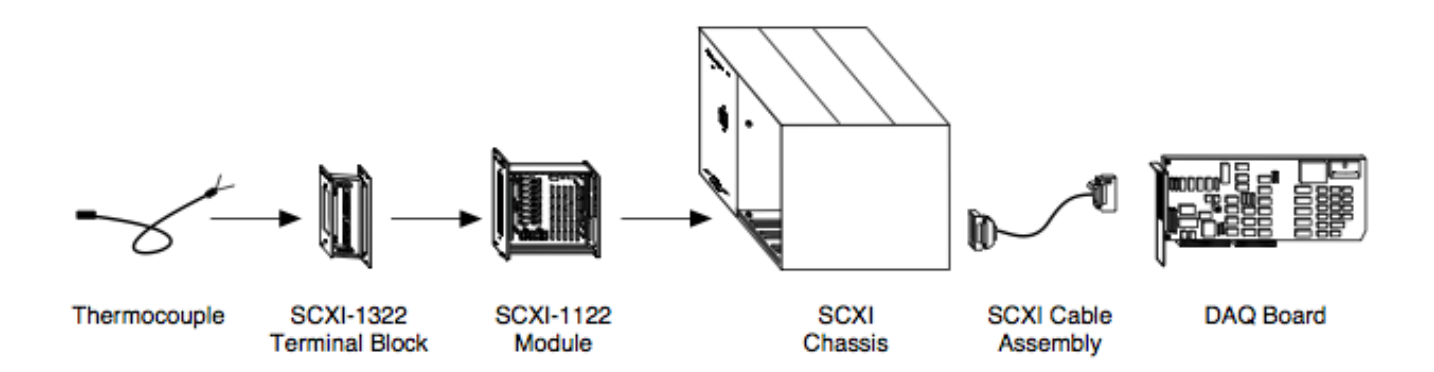


Figure 3-3 DAQ system configuration diagram (National Instruments , 1996, p.2)

## 4 Results

## 4.1 Standard consistence and time of setting

An analysis of the results obtained from the SANS 50196-3 (2006) standard test method follows.

#### 4.1.1 Standard consistence test

The w/b ratios for the experimental mixtures were determined through the standard consistence test, which was conducted as described in section 3.2. The results of the test are presented in the table below.

Table 4-1 w/b ratio at standard consistence and corresponding Blaine fineness

Standard consistence test - SANS 50196-3				
Mixture w/b Blaine fineness (m²/kg)*				
M1 - PC	0.28	346 (100 % CEM I 52.5 N)		
M2 - BS	0.31	390 (100% GGBS)		
M3 - CS	0.31	467 (100%GGCS)		

\*Note: The Blaine fineness values for the slags were taken from Research Monograph 6 (Alexander et al., 2003) and value for the PC (CEM I 52.5 N) was acquired from PPC directly (Jones, 2012).

The variation in water required between the 100% PC paste and the slag pastes could be attributed to the increased cohesion related to the fineness of slag, but the finer Corex slag did not differ in water requirements to blastfurnace slag to achieve a standard consistence. Although Alexander et al. (2003) mention that the workability and pumpability of Corex slag concretes do not significantly differ from PC concrete and that slag concretes generally have slightly lower water demands. However consistency as described by Kellerman and Crosswell (2009) is the mobility or ease of flow related to the wetness or dryness of the mix and in general wet concrete is more workable than dry concretes, but they go on to say that concretes of the same consistence may vary in workability. It is also important to mention that the consistence test was conducted on pastes and therefore may not be directly comparable to concrete.

#### 4.1.2 Initial and final setting time

The results of the test, which can be seen in Table 4-2 on the following page, clearly indicated that slag increases the initial and final setting times, but no clear difference in initial time of set was seen between Corex slag and blastfurance slag. However Corex slag did reach final set 30 min faster than blastfurnace slag, which shows that Corex slag appears more reactive as indicated by Alexander et al. (2003). Furthermore the lag between initial and final set increased by around 25-55 min with the addition of slag, which could be attributed to the lower rate of reaction of slag and water.

Jaufeerally (2002) conducted the same setting time test (SANS 50196-3, 2006) with Corex slag and blastfurnace slag but used a different cement with a lower strength class (CEM I 42.5 N). He found that Corex slags had slightly longer initial setting time but shorter final time of set at a replacement level of 50%, when compared to blastfurnace slag. A comparison of these results to those measured using CEM I 52.5 N revealed the following variations:

- CEM I 52.5 N took longer to reach initial setting time but no clear difference in final setting time was found
- Blastfurnace slag had a slightly longer initial setting time but more rapidly reached final time
- Corex slag decrease in both initial and final setting times

No clear relationship can be drawn from this comparison other than the apparent decrease in final time of set of slag paste when CEM I 52.5 N cement is used. The setting times measured by Jaufeerally (2002), at 50% replacement, as well as the variations from CEM I 52.5 N can be seen in Table 4-3 below.

Table 4-2 Initial and final setting times of experimental mixtures

Setting time test - SANS 50196-3 (min)				
Mixture	Initial	Final		
M1 - PC	200	255		
M2 - BS	250	360		
M3 - CS	250	330		

Table 4-3 Setting time results with CEM I 42.5 N and variation from CEM I 52.5 N (Jaufeerally, 2002)

Setting time test - SANS 50196-3 (min)					
Mixture	Mixture Initial Variation Final Variat (CEM I 42.5) (CEM I 42.5)				
100% - PC	170	30	255	0	
50% - BS	230	20	405	(40)	
50% - CS	270	(20)	355	(25)	

\*Note: Brackets indicate a decrease

# 4.2 Semi-adiabatic calorimetry

The thermal measurements obtained from the custom-built low budget semi-adiabatic calorimeter are presented over a 24 h period. Thermal measurements commenced within 6 min 30 sec of wetting the binder. Due to this time delay the initial peak, which is followed by a rapid decrease in heat rate, was not captured. Two measurements of each sample mixture were taken and the average difference between samples of the same mix at equivalent times was  $\pm 0.24$  °C and the inert samples fluctuated within the range of  $\pm 3$  °C. The signal to noise ratios (see section 2.4.4) can be seen in the table below.

Table 4-4 Signal-to-Noise ratio of the experimental mixers

Signal-to-Noise Ratio*				
Mixture	Ratio	limit		
M1 - PC	16.05	>5		
M2 - BS	20.2	>5		
M3 - CS	19.9	>5		

<sup>\*</sup>Note: See Figure 2-16 on page 30 for a graphical illustration of how the signal and noise quantities were determined.

Over all the semi-adiabatic calorimeter met the specifications outlined in the ASTM draft standard (2012).

#### 4.2.1 Temperature profiles

The temperature profiles of the three experimental mixtures, as well as the corresponding inert profiles, where plotted directly from the data obtained from the semi-adiabatic system and can be seen in Figure 4-2 on page 46. The temperature profiles were similar in shape to examples presented in the ASTM draft standard (2012) for mixtures of similar mass and insulation and example from this draft can be seen in Figure 4-1 on the following page. The temperature profiles in Figure 4-2 clearly indicate that pastes made with slag (GGBS and GGCS) have the effect of decreasing and delaying the main peak response and lowering the rate of increase of temperature, relative to 100% PC.

Table 4-5, on the following page, shows the maximum temperature reached by the mixtures and the corresponding time, as well as the percentage change from 100% PC. In the case of Corex slag a higher maximum temperature was reached at a greater shift than that of blastfurnce slag, which confirms the results that Alexander et al. (2003) reported with the exception of Corex slag having an appreciable decrease in the heat evolved (based on the temperature differential) when compared to the 100% PC sample. This result could be attributed to the use of a more reactive PC of a higher strength class (CEM I 52.5 N) but the fact that thermal measurements were conducted on paste samples as opposed to concrete samples may present a bias. However the introduction of 50% Corex slag results in a 32% reduction in the maximum temperature reach by 100% PC paste and caused an 87% increase in the time at which the peak was reached. The thermal behaviour of the experimental mixtures will be discussed further in section 4.2.2 where the heat profiles are compared.

Table 4-5 Peak temperature and the percentage change from 100% PC due to GGBS and GGCS additions

Peak Temperature					
Mixture	Peak Temp (°C)	Change (%)	Time (h)	Shift (%)	
M1 - PC	83.42	-	10	-	
M2 - BS	45.19	(46)	13	30	
M3 - CS	56.76	(32)	18	80	

**Note:** Brackets indicate decrease

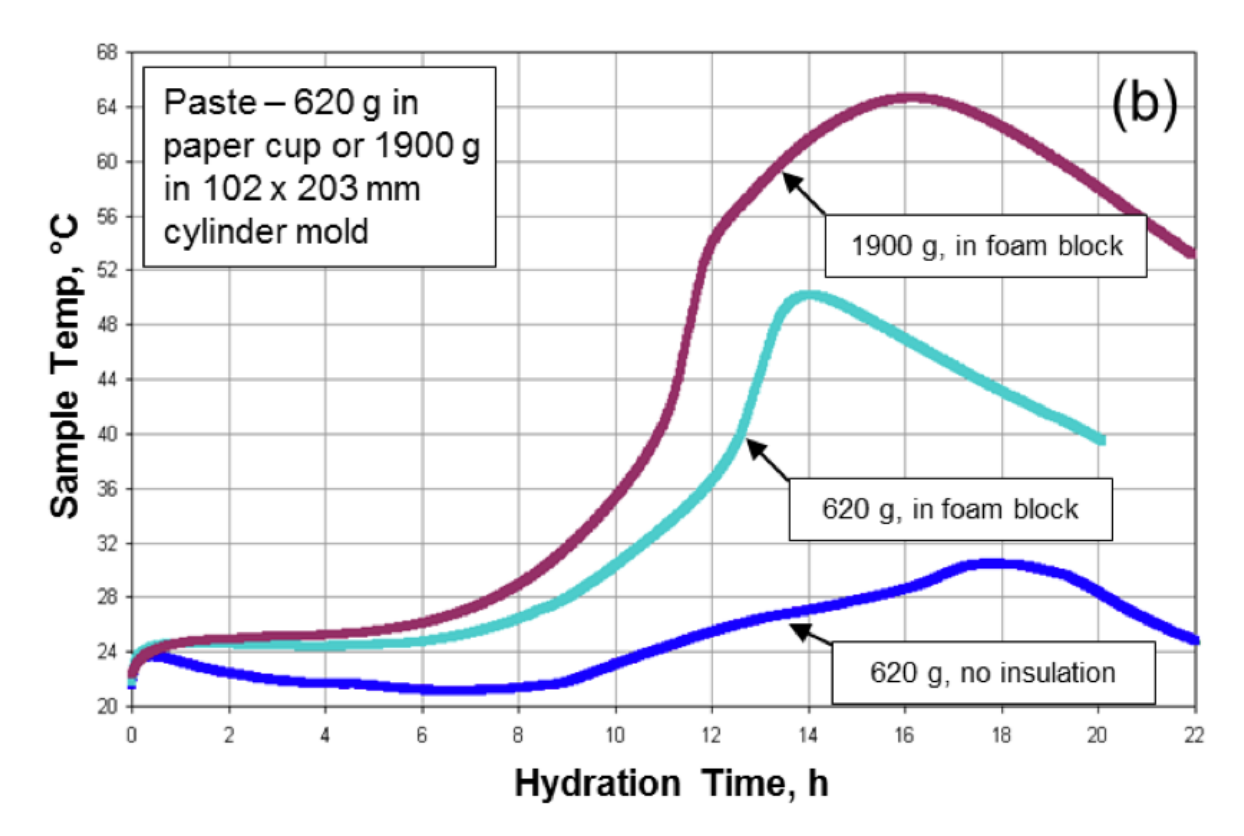


Figure 4-1 Effects of varied insulation and sample mass on repeated paste mixtures (ASTM draft, 2012, p.25)\*

**Note:** The mixtures featured in Figure 4-1 were made using CEM I with 25% Class C fly ash and Type A water reducing admixture at a w/b ratio of 0.51.

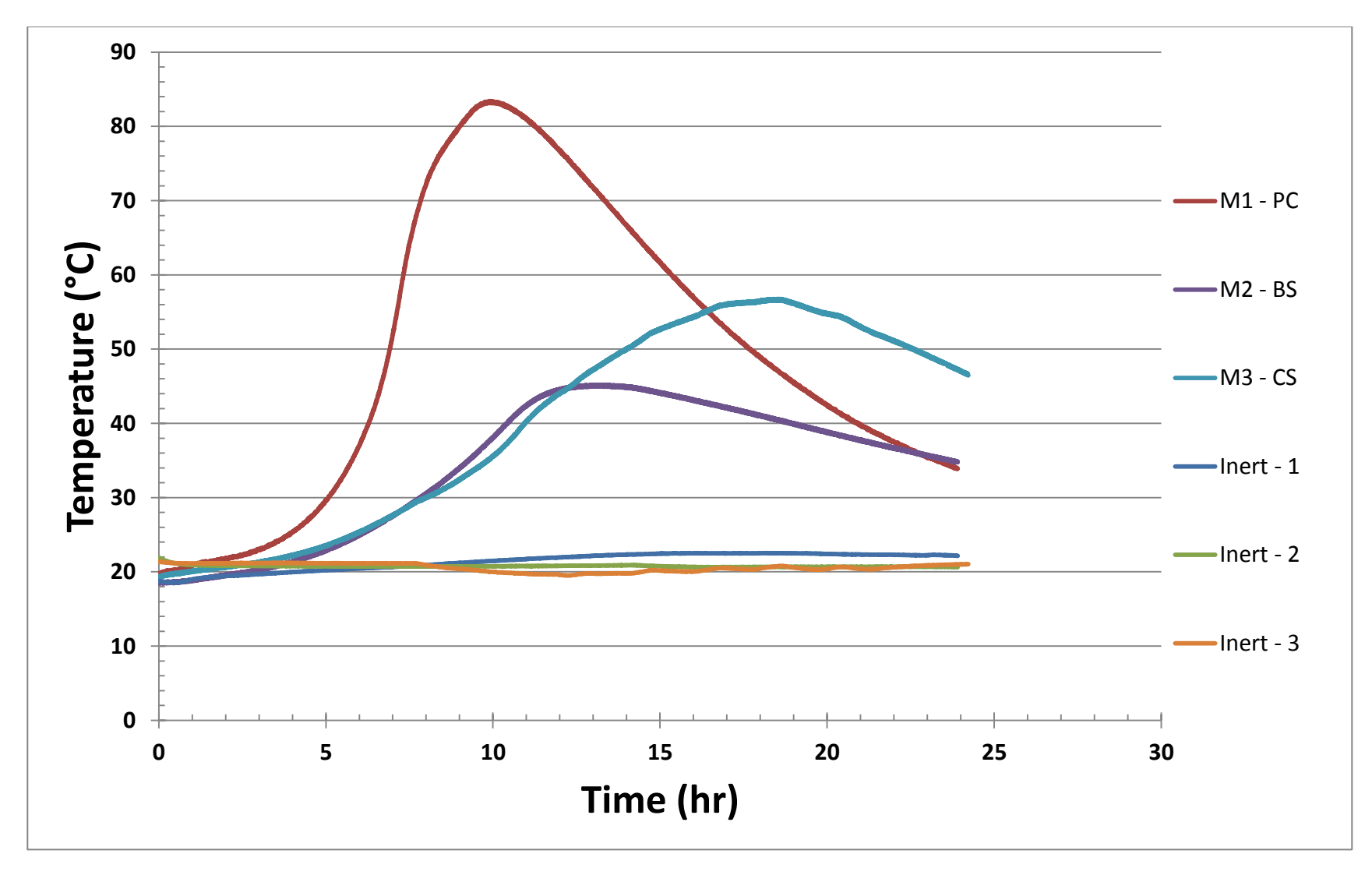


Figure 4-2 Temperature profiles of experimental mixtures and the corresponding inert profiles

Note: The raw data can be downloaded from the following link - https://www.dropbox.com/sh/qjaso9scaf6kkdb/RO\_jonN6jW

#### 4.2.2 Heat profiles

The heat evolved during the 24 h curing period was calculated by using equation 2-5 which approximates the heat evolved at any time per unit mass of binder. The specific heat capacity used in heat calculations was determined by the weighted average specific heat of the constituent materials, which has deemed sufficiently accurate for concrete (Ballim & Graham, 2009). The specific heat capacity of cement and cement extenders was taken as 880 J/kg.K and a value of 4187 J/kg.K was used for water, which was recommended by Ballim and Graham (2009). The temperature change was determined by subtracting the temperature of the inert sample from the active sample at the equivalent time. The 24 h heat cures, which can be seen in Figure 4-3 on the following page, do not give further insight into the behaviours of the mixtures when compared to the temperature profiles, however the quantity of heat generated over time may be assessed against the heat profiles developed by Alexander et al. (2003) for mixtures of the similar constituents. Although the heat profiles developed by Alexander et al. (2003) differ by the following:

- CEM I 42,5N was used as opposed to CEM I 52.5N
- A high w/b ratio was used
- The calorimetric system used was classified as fully adiabatic
- Concrete mixtures were measure as opposed to cement pastes
- Larger volume samples were measured

In spite of these differences the w/b ratio has little effect on the heat released during the first 12 h of testing (Bentz et al., 2009) and the temperatures measured during the first few hours (approximately 10 h) are relatively independent of the calorimetric method used (Weakley, 2010), although the level of insulation for the semi-adiabatic system needs to be considered to prevent excessive heat losses. However test presented in the ASTM draft standard (2012) revealed that concrete mixture had lower heat development then pastes and samples of larger mass produce elevated profiles. A comparison between the heat profiles can be seen in Figure 4-4 on page 49.

The comparison showed that 100% CEM I 52.5 N had greater heat development between 5 to 12 hours, after wetting of binder, even after heat losses from the semi-adiabatic system took affect at the 9 h mark. This clearly indicates that the higher strength class cement has a significant effect on the heat liberated during the hydration reaction. Although this comparison is between a cement paste and a concrete mix, and therefore, a test with samples of cement paste (or concrete) at equivalent mass would need to be conducted to eliminate this bias. The 50% blastfurnace slag mixture showed a similar behaviour to that found between the 100% PC mixtures, however the 50% Corex slag mixture had a similar trajectory before heat losses took affect at the 13 hour mark, revealing no apparent difference, which is unexpected due to the higher strength cement used in the mixture.

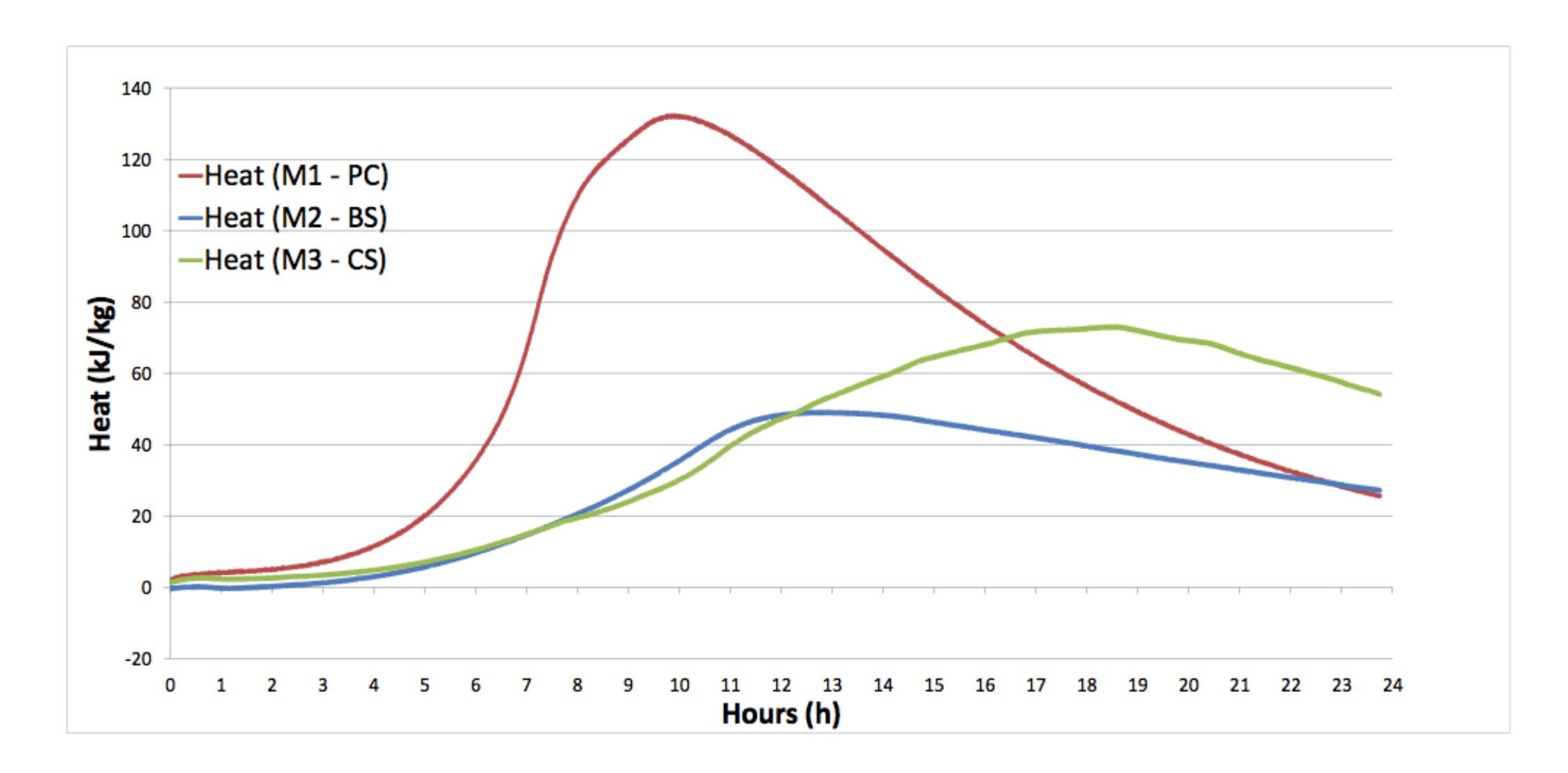
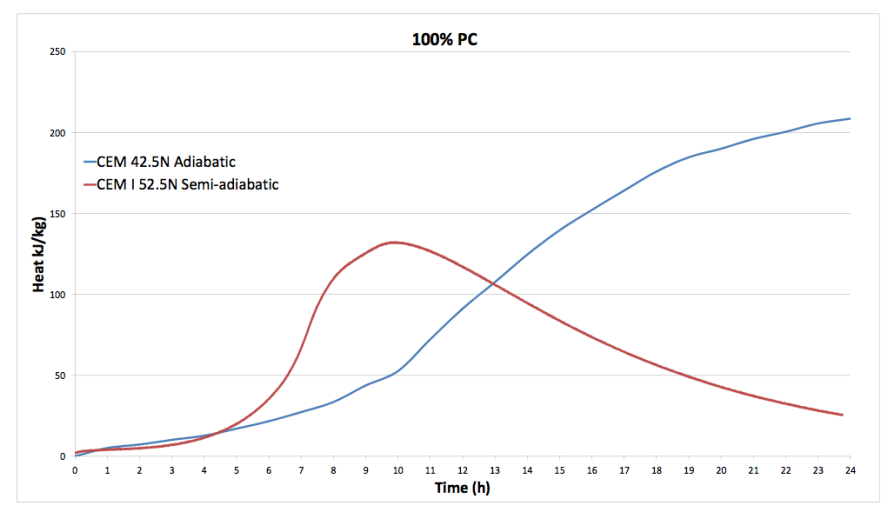
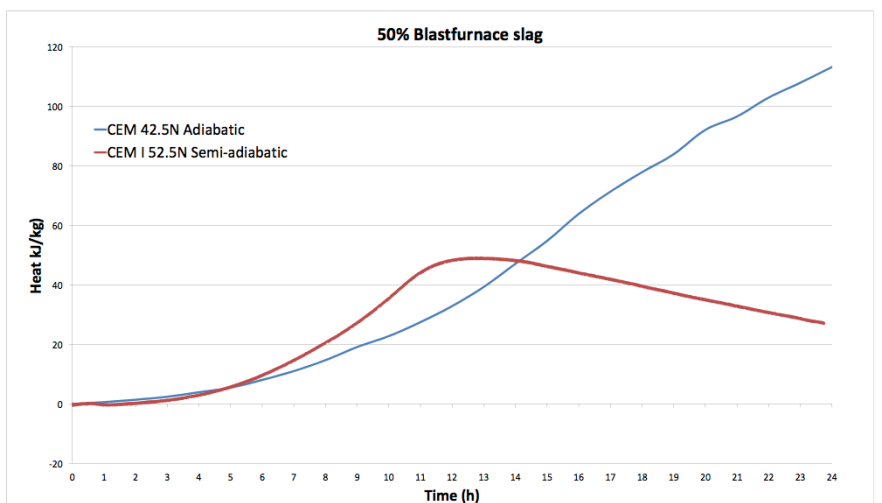


Figure 4-3 Heat profiles for experimental mixtures





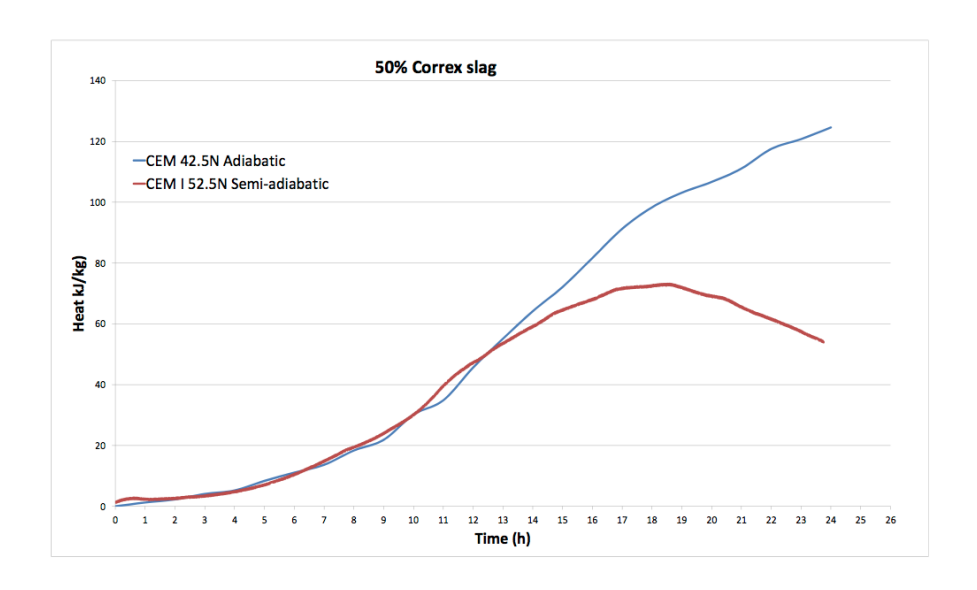


Figure 4-4 Heat profile comparison between CEM I 42.5N and CEM I 52.5N with slag addition, measured by fully adiabatic calorimetry and semi-adiabatic calorimetry respectively\*

\*Note: The CEM I 42.5 N heat profiles were extracted from Figure 2-6 for the first 24 hours (Alexander et al., 2003)

#### 4.2.3 Rate of heat evolution

The heat rate profiles were developed by means of numerical differentiation with respect to time of the heat curves in Figure 4-3 and are presented in Figure 4-5 on the following page. The rate at which heat is liberated directly indicates the rate at which the exothermic reaction is taking place. The 100% PC mixture displayed a higher peak heat rate compared to the two slag mixtures, which was expected, however the slags also showed a significant increase in the time to reach peak heat rate ( $\approx 4$  h). This finding contradicts observations made by Ballim and Graham (2008) who found blastfurnace slag to reduce the time to reach peak **heat rate** when in combination with CEM I 42.5 N. The Corex slag mixture appears to react over a longer time period to that of blastfurnace slag; however no appreciable difference in peak heat rate can be observed. The table below shows the peak heat rates and the corresponding times for the three experimental mixtures, as well as the percentage change between from 100% PC.

Table 4-6 Peak heat rates and the percentage change from 100% PC due to slag addition

Peak Heat Rate					
Mixture	Peak Heat Rate (W/kg)	Change (%)	Time (h)	Shift (%)	
M1 - PC	1.21	-	8	-	
M2 - BS	0.25	(82)	10.8	35	
M3 - CS	0.27	(80)	11.2	40	

A relative comparison between the experimentally measured profiles (heat and heat rate) and those produced by Alexander et al. (2003) are presented in Figure 4-6 on page 52. A direct comparison cannot be made due to the differences mentioned in Section 4.2.2, however the relative comparison may be useful in establishing general trends. From this comparison the 100% CEM I 52.5 N pastes shows a higher degree of heat evolution at a faster rate than that of CEM I 42.5 N within the first 10 hours. Although the introduction of slag to CEM I 52.5 N significantly reduced the heat generated and the rate at which it developed. However when an analysis is made between the slag mixtures the variation in the strength class of the cement used reveals comparatively minor differences in the profiles over a 24 h period.

From this observation CEM I 52.5 N displays a high degree of reactivity but is heavily influenced by the addition of blastfurnace slag and Corex slag. This may indicate an incompatibility between the slag and the PC at a 50% replacement level. However the low w/b ratio used in the experimental mixtures coupled with bleeding during the thermal measurements may have affected the ability of the slag to completely react. The air gap created between the sample flask lid and the sample surface ( $\approx$  100 ml) may have allowed for excessive bleeding. This could ultimately result in an inadequate amount of water available to sufficiently allow for the slag to react especially as slag is a latent hydraulic binder and relies on the Ca(OH)<sub>2</sub> produced due to the hydration of PC. Based on a model presented by Grieve (2009) a cement paste with a w/b ratio under 0.4 will not have sufficient water to allow for complete hydration of the available cement and approximately 15% of the binder will not react for a w/b ratio of 0.31, which was the w/b used for the slag mixtures.

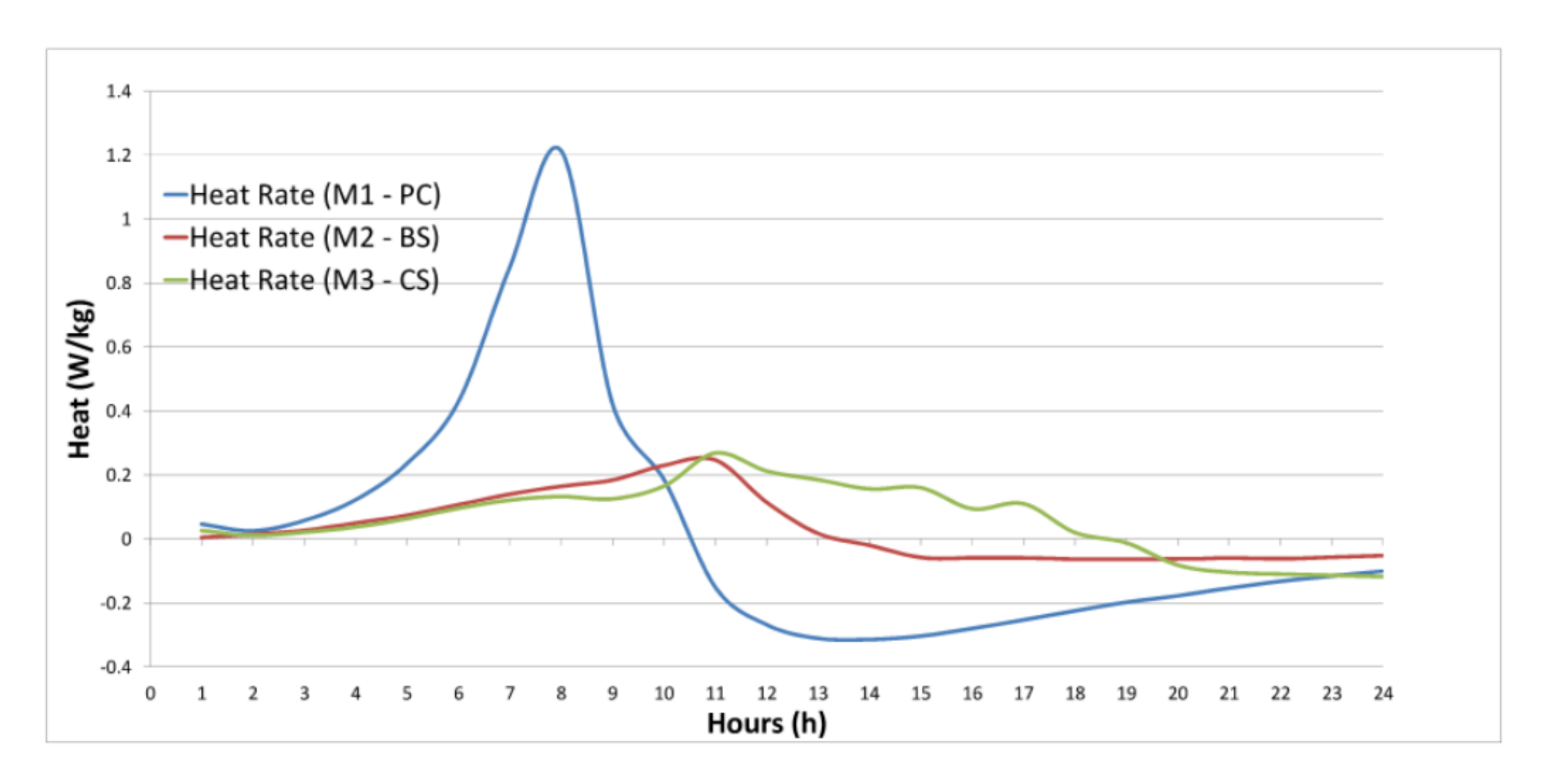
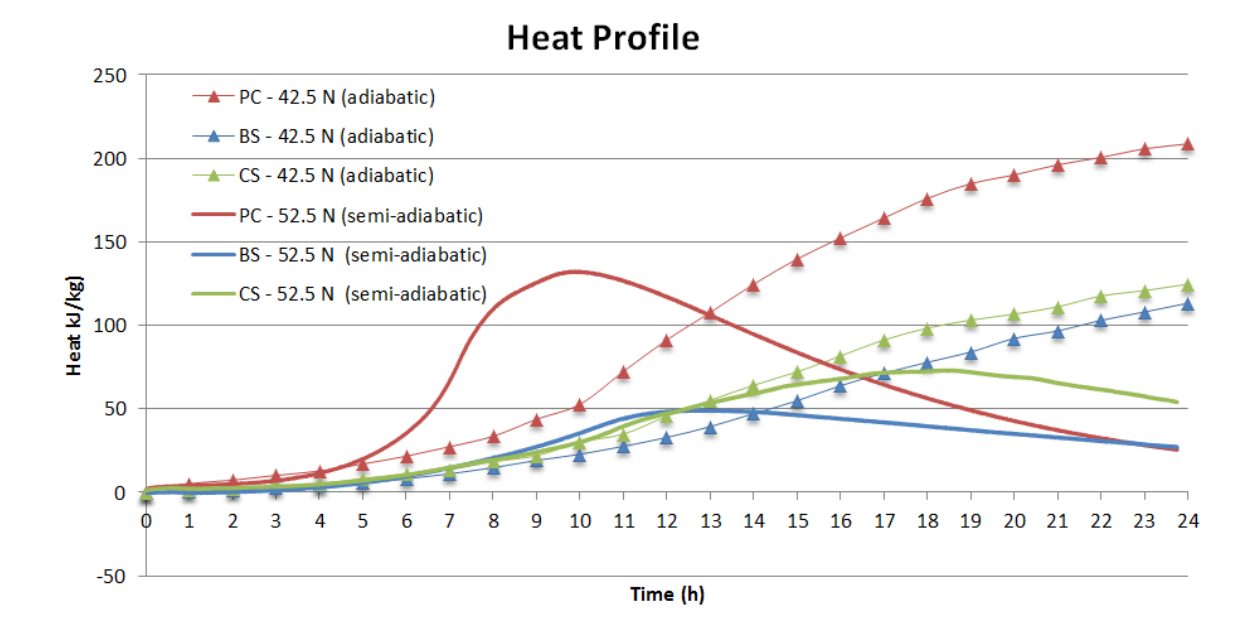


Figure 4-5 Heat rate profiles of experimental mixtures



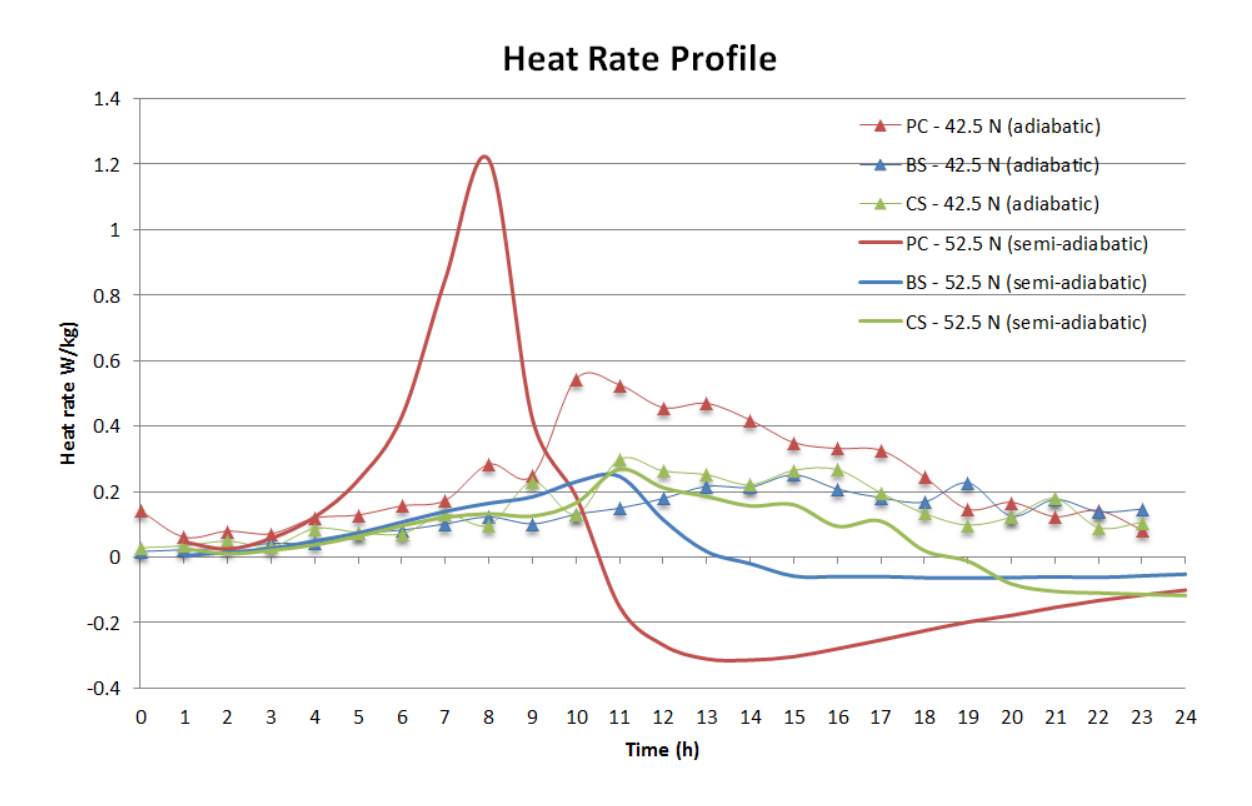


Figure 4-6 Profile comparison between CEM I 42.5N and CEM I 52.5N with slag addition (GGBS and GGCS), measured by fully adiabatic calorimetry and semi-adiabatic calorimetry respectively\*

\*Note: The CEM I 42.5 N heat profiles were extracted from Figure 2-6 (Alexander et al., 2003) for the first 24 hours and the heat rates were approximated by numerical differentiation of the heat curves developed.

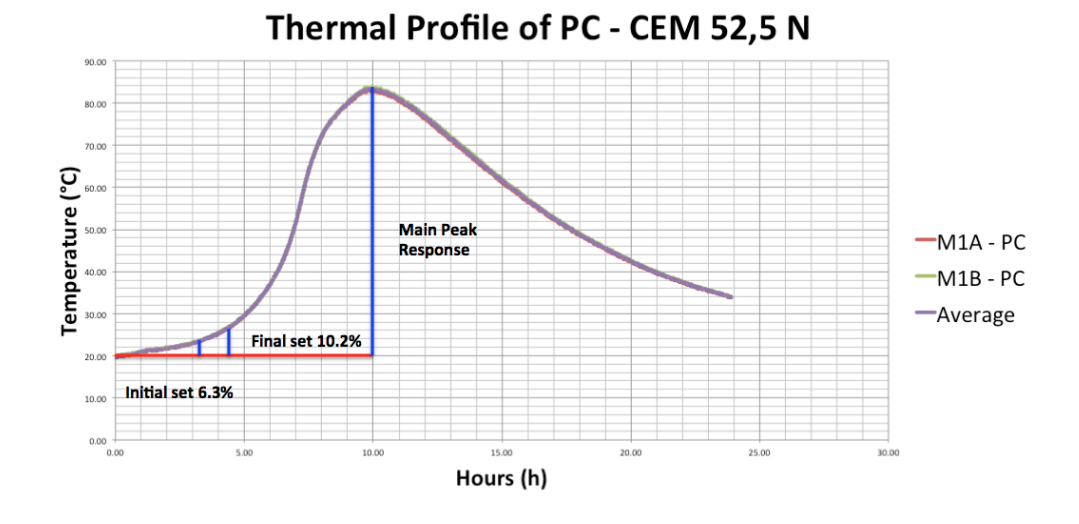
## 4.3 Temperature profile and setting time relationship

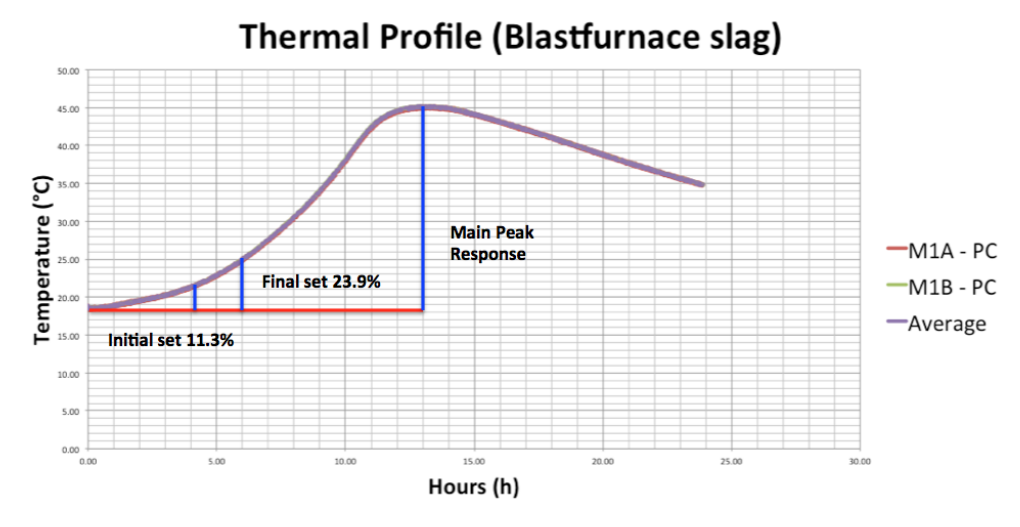
The setting times of the mixtures determined by SANS 50196-3 (2006) were compared to the corresponding thermal profile in order to determine any relationships between the main peak response (MPR) and initial and final setting times (see section 2.4.4). Table 4-7 below shows what proportion of the MPR, developed by the temperature profiles, correlate with the established setting times. After comparing the results no clear correlation between the setting times and a specific fraction of the MPR for the cement pastes was found. The ASTM draft standard (2012) recommends fractions of 20% and 50% for initial and final setting times respectively, but indicates that this proportioning is for mortars that are wet sieved from a concrete mixture. The draft standard does mention that when pastes of similar proportions are substituted for mortar and the same % fraction compared, the associated thermal indicators in general overestimate setting times. This appears to be the case in this instance due to the low % fractions calculated from the results, although mortars would need to be tested to validate this claim. The fractions calculated from the experimental mixtures fall below 20% and 50% for initial and final setting times respectively, however no clear set fraction is identified as the variations are too large to produce a defined relationship. Although the blastfurnace slag mixture appears to be the outlier as the 100% PC showed relatively small variations for initial (2.2%) and final (4.6%) setting time fractions when compared to the Corex. Figure 4-7 on the following page shows the thermal profiles with the setting time markers indicated on the profile.

In an evaluation of the fractions method of determining setting time Weakley (2010) noted that minimal insulation was provided and no adjustment was made for thermal losses, and therefore, this method is heat-loss and device dependent. Taking this into account the low fractions of the MPR that were found could have been due to the relatively high level of insulation provided in an attempt to limit heat losses. It appears that this method for determining setting times was developed for simple and inexpensive thermal measurement methods at low levels of insulation.

Table 4-7 Proportion of main peak response corresponding to initial and final setting times for temperature profiles

Proportion of MPR corresponding to setting times					
Mixture Initial set Proportion of MPR (%) Final Set Proportion of MPR (%)					
100% - PC	200	6.3	255	10.2	
50% - BS	250	11.3	360	23.9	
50% - CS	250	8.5	330	14.8	





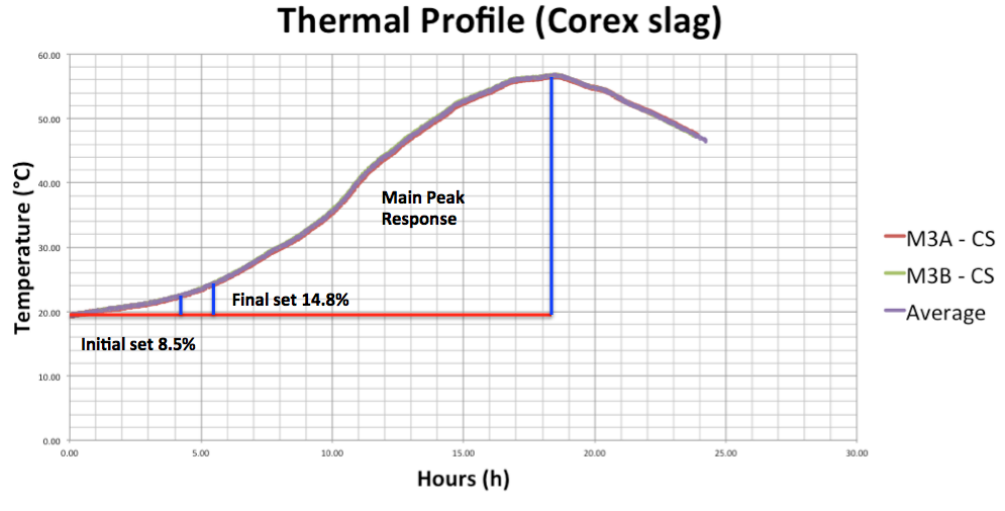


Figure 4-7 Temperature profiles of experimental mixtures with setting time makers shown at initial and final setting times\*

\*Note: For each temperature profile two samples of the same mixture where plotted along with the average

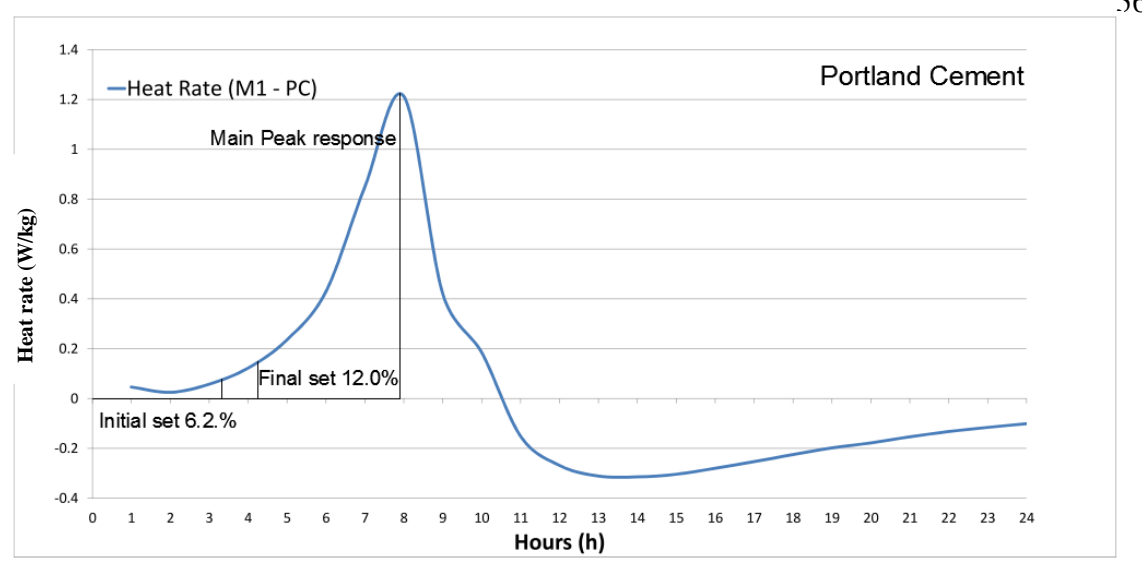
# 4.4 Heat rate profile and setting time relationship

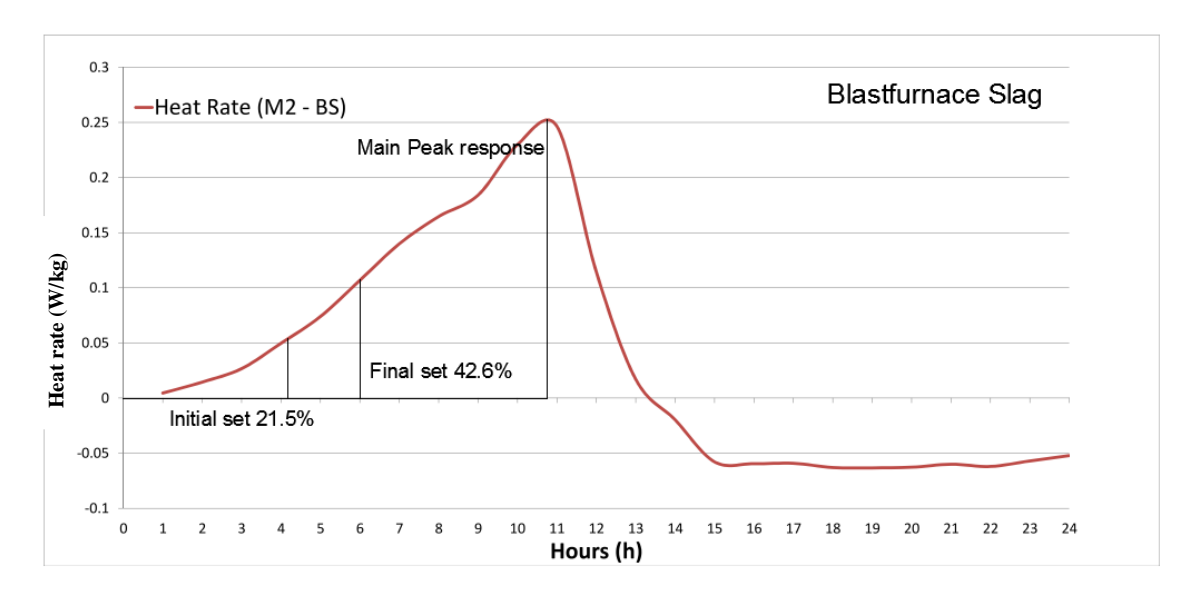
The heat rate profiles were also assessed with regard to setting time as the rate of heat evolution directly relates to the extent of the exothermic reaction. The assessment was conducted in the same manner as the temperature profiles, where the proportions of the MPR corresponding to the measured setting time were evaluated. The assessment is graphically represented in Figure 4-8 on the following page and a summary is provided in Table 4-8 below. No clear proportion was found that related to all the samples, however the initial setting time proportions were approximately half the final setting time proportions for all three mixtures.

The fractions method of setting time, by semi-adiabatic calorimetry, may be useful for quality control if the thermal profiles of the specific mixtures in question have been calibrated against a direct setting time test. However the system would need to be monitored for excessive heat losses and the level of insulation would need to be optimised during calibration. No insulation is provided for samples during setting time tests and therefore the reaction rate may vary from that of an insulated sample. The low fractions measured could be as a result of excessive insulation, which produced amplified peaks in the profiles. Methods of calorimetry that produce more consistent thermal profiles, such as isothermal and fully adiabatic systems, may be more useful in developing direct relationships for predicting cement and concrete characteristics.

Table 4-8 Proportion of main peak response corresponding to initial and final setting times for heat rate profiles

Proportion of MPR corresponding to setting times					
Mixture	Initial set	Proportion of MPR (%)	Final Set	Proportion of MPR (%)	
100% - PC	200	6.2	255	12.0	
50% - BS	250	21.5	360	42.6`	
50% - CS	250	15.6	330	29.9	





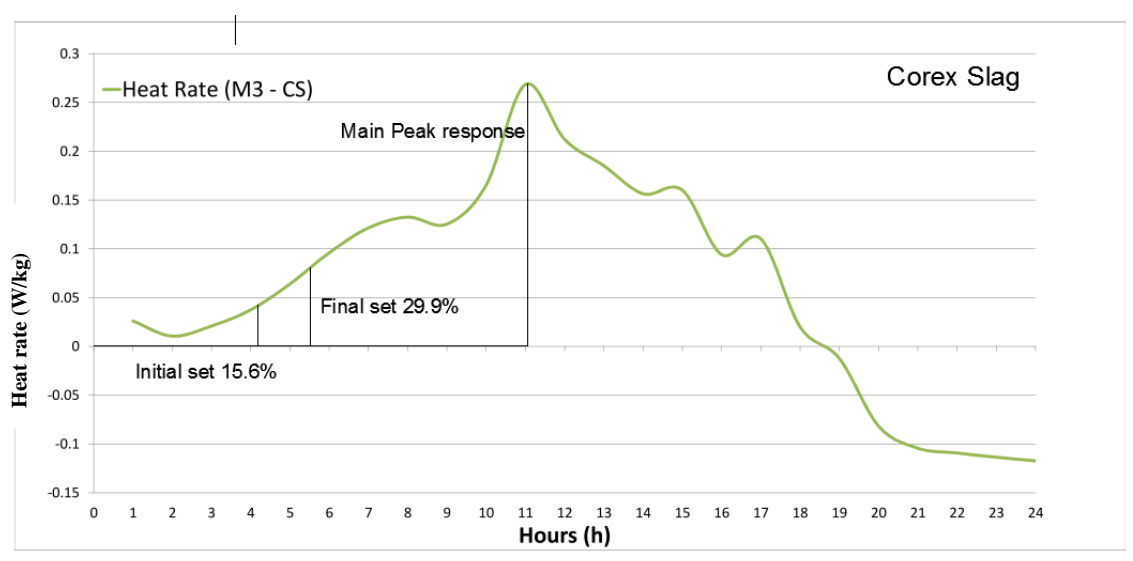


Figure 4-8 Heat rate profiles of experimental mixtures with setting time makers shown at initial and final setting times

## 5 Conclusions

## 5.1 Thermal properties of GGCS and GGBS

Ultimately the results indicate that slag pastes have lower rates of heat development and therefore may be beneficial in the reduction of thermal cracking in large concrete pours. Although Cores slag does not offer the same heat reduction benefit as blastfurnce slag, it still produced a 32% reduction in the peak temperature of 100% PC paste over a 24 hour period. This finding is contrary to results presented by Alexander et al. (2003), which indicated no appreciable reductions in the heat produced through Corex slag addition. However it is possible that the Corex mixture has a slower decrease in heat rate after the initial peak that occurs within 24 hours. This characteristic could lead to a total heat production that shows less severe differences between the Corex slag mixture and 100% PC mixture after a 7 day period. In order to validate this claim heat profiles would have to be developed over a longer time period with a fully adiabatic calorimeter to avoid heat loss.

## 5.2 Semi-adiabatic calorimetry

The semi-adiabatic calorimetric setup constructed and detailed in this report is a convenient and cost effective system as clear thermal profiles were developed and the thermocouples embedded in the samples could easier be retrieved for reuse. Semi-adiabatic calorimetry is still a relatively new means by which to monitor and characterise cements and concrete within industry, however it is growing and simply lacks standardisation and empirical evidence to support its use. The exothermic nature of the hydration reaction makes the measurement of the thermal profiles an insightful graphical tool to classify and characterise cements, blended cements and concrete mix designs. However semi-adiabatic calorimetry does not give clear indications of the actual heat liberated during the curing period and therefore cannot be used to develop input data for heat prediction model to monitor thermal cracking. Its use should be focused on comparative data but even in this case caution must be taken because there are many variables that may affect the results such as the level of insulation, sample volume and test environment. For this reason the accuracy of a calorimeter is an important parameter to be aware of even if comparative analysis is the key concern as the relative difference between two systems may result in analysis methods becoming invalid within a curtain accuracy level. One way to combat this problem is to establish a classification method for semi-adiabatic systems relative to a fully adiabatic system. A semiadiabatic system could be classified by comparing the results obtained for a standard mixture to those established by a fully adiabatic system. Comparative test methods may then be tailored to semi-adiabatic calorimeters that fall within a curtain classification. Ultimately a fully adiabatic calorimetry is important for developing quantifiable heat rate values for temperature prediction models for structural analysis. However more in-complex and cost effective semi-adiabatic systems are more useful for industry to adopt due to the robust nature and mobility that can be offered.

# 5.3 Setting time properties of GGCS and GGBS

There was a clear indication that slag addition increased both the initial and final setting times then compared to 100% PC. No clear difference was found between the initial setting times of Corex slag and blastfurnace slag; however the Corex slag did reach its final set 30 min faster, which verifies the increased reactivity. The use of CEM I 52.5 N also showed a decrease in final setting with both slags when compared to CEM I 42.5 N, which is expected due to the greater reactivity associated with a higher strength class of cement.

## 5.4 Relationship between thermal profile and setting time

The setting times of the experimental mixtures corresponded to very lower proportions of the main peak response. This could be attributed to the high level of insulation provided by the semi-adiabatic calorimetric setup and the low w/b ratios used for the mixtures. The level of insulation has been found to amplify the peak of the thermal profile (ASTM draft 2012), which in turn would result in smaller fractions of the MPR corresponding to setting time. Taking this into account isothermal calorimetry may be a better method for determining comparative characteristics because the level of insulation would not influence the profile developed as the heat generated is allowed to flow away from the sample providing consistent and reproducible profiles. However a semi-adiabatic calorimeter is far cheaper and easier to construct and a standard that explicitly specifies the level of insulation, sample volume, environment and temperature sensors required may eliminate the large degree of variability associated with is method of calorimetry.

# 6 Reference list

Alexander, M., Ballim, Y. & Mackechnie, J., 1999. *Research Monograph No. 4 - Concrete duribility index testing manual*. Monograph. Cape Town: Department of Civil Engineering University of Cape Town.

Alexander, M., Jaufeerally, H. & Mackechnie, J., 2003. *Monograph NO.6 - Structural and durability properties of concrete made from Corex slag*. Cape Town: University of Cape Town University of Cape Town.

ASTM draft, 2012. Evaluating hydration of hydraulic cementitious mixtures using thermal measurements. United States of America: Unpublished. Draft.

ASTM, 2008. Standard test method for time of setting of concrete mixtures by penetration resisteance. West Conshohocken: ASTM International ASTM.

ASTM, 2009. Standard Practice for Measurig Hydration Kinetics of Hydraulic Cementitious Mixtures Using Isothermal Calorimetry. West Conshohocken: ASTM International.

Ballim, Y., 2007. South Africa – Concrete construction industry – Cement based materials and civil infrastructure (CBM – CI). In *International Workshop - Cement Based Materials and Civil Infrastructure.*, 2007. unknown.

Ballim, Y. & Gibbon, G., 1996. Laboratory test procedure to predict the thermal behaviour of concrete. *SAICE Journal*, 38(3), pp.21-23.

Ballim, Y. & Gibbon, G.J., 1996. Laboratory test procedures to predict the thermal behaviour of concrete. *Journal of SAICE*, 38(3), pp.21-23.

Ballim, Y. & Graham, P., 2003. A Maturity Approach to the Rate of Heat Evolution in Concrete. *Magazine of Concrete Research*, 55(3), pp.249-56.

Ballim, Y. & Graham, P., 2005. A numerical model for predicting early age time-temperature profiles in large concrete structures. University of Cape Town.

Ballim, Y. & Graham, P., 2008. The effects of supplementary cementing materials in modifying the heat of hydryation of concrete. RILEM.

Ballim, Y. & Graham, P., 2009. Chapter 15 - Thermal properties of concrete and temperature development at early ages in large concrete elements. In G. Owens, ed. *Fulton's concete technology*. Midrand: Cement and Concrete Institute. pp.273-86.

Bamford, C. & Tipper, C., 1969. *Comprehensive chemical kinetics, Vol. 1: The practice of kinetics*. London: Elsevier Publishing Company.

Basyigit, C., Ozel, C. & Yucel, K.T., 2004. *Thermal insulation of expanded polystyrene as a construction and insulating material*. Isparta: Suleyman Demirel University Suleyman Demirel University.

Bentz, D., Peltz, M. & Winpigler, J., 2009. Early age properties of cement-based materials: II influences of water-to-cement ratio. *Journal of Materials in Civil Engineering*, 21(9), pp.512-17.

Cost, T., 2008. Practical Semi-Adiabatic Calorimetry for Concrete Mixture Evaluation. In *TTCC/NCC*., 2008. Holcim.

CP Tech Center, 2006. Developing a Simple and Rapid Test for Monitoring the Heat Evolution of Concrete Mixtures for Both Laboratory and Field Applications. Iowa: Iowa State University.

Fulton, 2012. Chapter 3 - Cementitious materials. In G. Owens, ed. *Fundamentals of concrete*. Midrand: Cement and Concrete Institute. pp.19-37.

Grieve, G., 2009. Chapter 1 - Cementitious materials. In G. Owen, ed. *Fulton's concrete technology*. Midrand: Cement and Concrete Institution. pp.1-16.

Jaufeerally, H., 2002. *Performance and properties of structural concrete made with Corex slag*. MSc (Eng) thesis. University of Cape Town.

Jones, M., 2012. *Riebeeck OPC Typical Analysis for Period April to June 2012*. [Document] Pretoria: Pretoria Portland Cement Available at: <a href="http://www.ppc.co.za">http://www.ppc.co.za</a> [Accessed 5 September 2013].

Kellerman, J. & Crosswell, S., 2009. Chapter 6 - Properties of fresh concrete. In G. Owens, ed. *Fulton's concrete technology*. Midrand: Cement and Concrete Institute. pp.83-94.

Kishore, K., 2010. *Mix Design with Superplasticizers*. [Online] Available at: <a href="http://www.engineeringcivil.com/mix-design-with-superplasticizers.html">http://www.engineeringcivil.com/mix-design-with-superplasticizers.html</a> [Accessed 20 October 2013].

Lechtman, H. & Hobbs, L., 1986. Roman Concrete and the Roman architecture relatution. In W.D. Kingery, ed. *Ceramics and Civilization Volume 3: High technology ceramics: past, present, future*. American Ceramics Society.

Mantel, D.G., 1994. Investigation into the hydraulic activity of fine granulated blastfurnace slags with eight different Portland cements. *Materials Journal*, 91(5), pp.471-77.

Naik, T., 1985. Maturity functions for concrete during winter conditions, Temperature Effects on Concrete. *American Society for Testing and Materials*, 858. ASTM STP 858.

National Instruments , 1996. *How to Use Thermocouples with an SCXI-1122 Module*. Application Note. National Instruments.

Owens, G., 2012. Chapter 3 - Cementitious materials. In G. Owens, ed. *Fundamentals of concrete*. Midrand: Cement and Concrete Institute. pp.19-37.

Roy, D., 1989. Fly ash and silica fume chemistry and hydration, Fly ash, silica fume, slag and natural pozzolans in concrete, Proceedings third international conference. *Special publication*, 114, pp.117-38.

SABS 196-3, 1994. *Methods of testing cement – Part 3: Determination of setting time and soundness.* Pretoria: South African Bureau of Standards.

SANS 10100-1:2000, 2000. *The structural use of concrete. Part 1: Design.* Pretoria: South African Bureau of Standards.

SANS 50196-3, 2006. *Methods of testing cement - Part 3: Determination of setting times and soundness.* Pretoria: South Africa National Standards.

SANS, 2006. *SANS 50196-1 - Method of testing cement - Part 1: Determination of strength.* Pretoria: South African National Standard South African National Standard.

Siemens VAI, 2013. *Corex*® *Technology*. [Online] Available at: <a href="http://www.industry.siemens.com/verticals/metals-industry/en/metals/ironmaking/corex/Pages/home.aspx#">http://www.industry.siemens.com/verticals/metals-industry/en/metals/ironmaking/corex/Pages/home.aspx#</a> [Accessed 20 September 2013].

Van Breugel, K., 1998. Prediction of temperature development in hardened concrete, Prevention of thermal cracking in concrete at early ages. 15, pp.51-75.

Weakley, R., 2010. *Evaluation of Semi-Adiabatic Calorimetry to Quantify Concrete Setting*. MSc Thesis. Alabama: Auburn University Auburn University.

# 7 Appendix A – Standard consistence and setting time experimental detail

The experimental procedure follows SANS 50196-3 (2006) and the apparatus and experimental procedure are detailed below.

# 7.1 Apparatus

This test is conducted with the use of a typical manual Vicat with attachments associated with standard consistence, initial setting and final setting times. A list of the required apparatus is as follows:

## Devices for preparing samples

- o Scale device accurate to 0.02g
- o Graduated cylinder (conforming to EN 196-1)
- o Mixer Hobart A120
- o Spatula

#### • Equipment to contain sample

- Truncated conical brass mould
- o Glass base place
- o Container for base plate and mould
- Mineral based oil

## Vicat Apparatus\*

- Standard Vicat
- o Plunger for standard consistence
- o Needle for initial set
- Needle with attachment for final set

\*Note: See Figure 2-21 on page 36 for a diagram of a typical manual Vicat apparatus

## 7.2 Procedure

#### The steps for mixing the cement pastes are as follows:

- 1. Experimental equipment must be set up in a lab with a control temperature of 20°C (±2) and relative humidity of no less than 50%
- 2. 500g of binder (in the desired proportions) along with the required quantity of water must be prepared and placed in the lab for 24h before testing to acclimatize to the lab temperature and relative humidity
- 3. The materials must then be placed into a mixing bowl and positioned under the automatic mixer <sup>1</sup>
- 4. Mixing commences directly after the require water quantity is added to the mixing bowl and the time of wetting must be recorded
- 5. Mixing takes place at a low speed and is stopped after 90s for 30s during which the paste adhering to the sides and bottom of the mixing bowl must be brought to the middle of the mixing bowl, after which a further 90s of mixing commences

- 6. Once mixing is completed the paste must immediately be transferred to the lightly oiled mould, which has previously been placed on a lightly oiled base-plate and filled to excess
- 7. Voids are to be removed by gently tapping the slightly overfilled mould against the ball of the hand
- 8. Excess paste is removed by a gentle sawing motion with a straight-edged instrument to leave the mould filled with a smooth upper surface.

#### The steps for determining standard consistence are as follows:

- 1. Secure the plunger to the Vicat apparatus and zero the scale by placing the plunger against the base plate. (Done prior to mixing cement paste)
- 2. Immediately after levelling the paste transfer the mould and base-plate under the Vicat apparatus so that the sample is centrally under the plunger
- 3. Gently low the plunger until it is in contact with the paste
- 4. Pause in this position (1-2 seconds) before releasing the plunger to penetrate the paste<sup>2</sup>
- 5. Read the scale 5s after penetration has ceased or 30s after the release of the plunger, whichever is earlier
- 6. Record the distance from the scale and the w/b ratio of the prepared sample
- 7. Repeat the experiment with cement pastes of varying w/b ratios until the distance between the plunger and base-plate is found to be 6 mm (±2 mm)
- 8. Once this distance is achieved record the water content to the nearest 0.5% as the water for standard consistence

#### The steps for determining initial setting time are as follows:

- 1. Fit the Vicat apparatus with the initial set needle and zero the scale by lower the needle until it is in contact with the base plate, after which raise the needle to the standby position
- 2. Place the filled mould and base-plate into the container and add water until the surface of the paste is submerged to a depth of at least 5mm, after which place the container into an environment of  $20 \pm 1$  °C  $^3$
- 3. After a suitable time (approximately between 160 260 min), position the mould, base-plate and container under the needle of the Vicat apparatus
- 4. Gently lower the needle into contact with the paste and pause (1-2 seconds) before releasing the needle to penetrate the paste and record the scale once penetration has ceased or 30s after release, whichever is earlier
- 5. Repeat this penetration process at conveniently spaced positions, not less than 8mm from the rim of the mould or 5mm for from the other penetrations point, and at least 10mm from the point of previous penetration
- 6. Conveniently spaced intervals of time (e.g. 10 min intervals), should be kept between penetrations and the needle must be cleaned between intervals
- 7. The initial time of setting is determined when the distance between the needle and the base-plate is 6mm (±3 mm) and the time is recorded from the time of wetting and rounded to the nearest 5 min

8. Retain the sample for determination of final setting and place in the controlled environment.

#### The steps for determining final setting time are as follows:

- 1. Fit the needle with ring attachment to the Vicat apparatus and zero the scale by lowering the needle to the base-plate, after which raise the needle to the standby position
- 2. Invert the filled mould of the sample used in initial setting time test and place it back onto the base-plate
- 3. After a suitable time (approximately between 245 345 min) place the mould, base-plate and container centrally under the Vicat apparatus
- 4. Gently lower the needle until contact is made with the paste and pause for 1-2 seconds before releasing the needle to penetrate the paste
- 5. Read the scale when penetration has ceased or 30s after the release of the needle, whichever is earlier
- 6. Repeat the penetrations at conveniently space positions of not less the 8mm from the rim of the mould or 5mm from previous penetrations, and at least 10mm from last penetrated position
- 7. Conveniently spaced time interval (e.g. 30 min spaced intervals), should be kept between penetrations, during which the needle should be cleaned
- 8. The final time of setting is determined when the ring attachment fails to mark the surface of the paste (needle penetration of 0.5 mm into paste) and the time is recorded from the time of wetting and rounded to the nearest 15min
- 9. The final time of setting may be confirmed by repeating the test in two other positions.

#### \*Notes:

- 1. The mixer used was a Hobart A120 which conforms to SANS 50196-1 (2006)
- 2. The release of the plunger must occur  $4\min \pm 10s$  after time of wetting for consistence test
- 3. The w/b ratio for the cement paste samples are determined by the consistence test and prepared in the same manner.

# 8 Appendix B – Semi-adiabatic calorimetric experimental procedure

The apparatus and procedure follow to measure the temperature profiles of cement paste mixtures is detailed below.

## 8.1 Apparatus

The apparatus used to conduct the experiment are listed below:

#### • Devices for preparing samples

- o Scale device accurate to 0.02g
- o Graduated cylinder
- o Mixer Hobart A120
- o Spatula

#### Insulation

- o Polystyrene flasks (450ml)
- o Polystyrene enclosure

## • Data Acquisition system (National Instruments)

- Workstation PC
- o NI SCXI-1000 Chassis
- o NI SCXI-1122 Channel Multiplexer
- o NI SCXI Cable Assembly
- o NI DAQ Board

#### • Software

- OS Windows 7
- o Program LabVIEW 2011

## • Thermal measurement equipment

- o NI SCXI-1322 Temperature sensor block
- o Type K thermocouples\*

\*Note: The thermocouple specifications are as follows:

- Grounded Type K sensor
- Diameter (D): 6mm
- Length (L)): 100mm
- Tolerance class 2 (±2.5°C)
- Max temperature of 350°C

### 8.2 Procedure

The steps of the experimental procedure undertaken are as follows:

- 1. Experimental equipment must be set up in a lab with a control temperature of 20°C (±2) and relative humidity of no less than 50%.
- 2. Materials must be prepared, based on the mix proportions (see Table 3-1), to produce a mixture volume of approximately 1.5 kg, after which the materials must be placed in the lab for 24h before testing to acclimatize to the lab temperature and relative humidity
- 3. The inert sample of sand and water, with approximately equivalent mass and volume to the test samples, must be prepared and placed into insulated enclosure before the mixing of cement paste commences
- 4. The materials must then be placed into a mixing bowl and positioned under the automatic mixer <sup>1</sup>
- 5. Mixing commences directly after the require water quantity is added to the mixing bowl and the time of wetting must be recorded <sup>2</sup>
- 6. Mixing takes place at a low speed and is stopped after 90s for 30s during which the paste adhering to the sides and bottom of the mixing bowl must be brought to the middle of the mixing bowl, after which a further 90s of mixing commences
- 7. The batched content is then transferred to two polystyrene flasks (450ml each) and placed on a vibration table for 10s to consolidate
- 8. The samples are then weighed to ensure a mass of 650g with a difference of no more than 5%
- 9. After consolidation the samples are placed, along with the inert sample, into the insulated enclosure at a spacing of 10cm apart
- 10. The thermocouples (Type K) are then fully submerged into the samples, after which the flash lids must be secured
- 11. Finally the thermal data collection system is activated and the time of initiation must be recorded (approximately 6 min 30 sec after time of wetting)
- 12. The acquisition of data is terminated after 24hrs and the data is extracted for evaluation
- 13. This procedure is repeated for all three mixture (M1-M3)

#### \*Note:

- 1. The mixer used was a Hobart A120 which conforms to SANS 50196-1 (2006)
- 2. The w/b ratio for the samples is determined by the consistence test